

DISCUSSION PAPER SERIES

IZA DP No. 18176

The Immediate and Lasting Effects of Heat Waves on Workers

Hannah Klauber Nicolas Koch Nico Pestel

OCTOBER 2025



DISCUSSION PAPER SERIES

IZA DP No. 18176

The Immediate and Lasting Effects of Heat Waves on Workers

Hannah Klauber

Potsdam Institute for Climate Impact Research

Nicolas Koch

Potsdam Institute for Climate Impact Resesarch and IZA

Nico Pestel

Maastricht University and IZA

OCTOBER 2025

Any opinions expressed in this paper are those of the author(s) and not those of IZA. Research published in this series may include views on policy, but IZA takes no institutional policy positions. The IZA research network is committed to the IZA Guiding Principles of Research Integrity.

The IZA Institute of Labor Economics is an independent economic research institute that conducts research in labor economics and offers evidence-based policy advice on labor market issues. Supported by the Deutsche Post Foundation, IZA runs the world's largest network of economists, whose research aims to provide answers to the global labor market challenges of our time. Our key objective is to build bridges between academic research, policymakers and society.

IZA Discussion Papers often represent preliminary work and are circulated to encourage discussion. Citation of such a paper should account for its provisional character. A revised version may be available directly from the author.

IZA DP No. 18176 OCTOBER 2025

ABSTRACT

The Immediate and Lasting Effects of Heat Waves on Workers*

This paper examines how prolonged exposure to heat affects the labor force's ability to work in the short and long run. Linking administrative public health insurance records for one-third of the German working-age population to the quasi-experimental occurrence of heat waves, we provide the first comprehensive characterization of the occupation-specific heterogeneity in how heat-induced health damages materialize in decreased labor supply, and its distributional implications. An average hot day increases the number of new sick leave cases, and the effects build with prolonged heat. After seven consecutive days of heat exposure, the impact is roughly three times greater than on the first day. Workers who are already disadvantaged in terms of their income and working conditions are more vulnerable to heat stress. Those who are more flexible in scheduling and adjusting their working hours are less at risk. Our results also reveal a longer-term decrease in labor supply in the years following heat wave exposure, and suggest sustained increases in expenditures for healthcare.

JEL Classification: J20, J32, I18, Q50

Keywords: heat, labor, inequality, climate change, adaptation

Corresponding author:

Nicolas Koch Potsdam Institute for Climate Impact Research (PIK) EUREF Campus 19 10829 Berlin Germany

E-mail: nicolas.koch@pik-potsdam.de

^{*} We thank Christian Günster and Thomas Ruhnke at AOK Research Institute (WIdO) for making our analysis possible and for providing invaluable advice on the insurance data. Additionally, we thank Joseph E. Aldy, Francesca Dominici, Moritz Drupp, Piero Basagali, Omar Martin Fieles-Ahmad, Andrew Ireland, Marcelo Goncalves, Felix Holub, Jörg Lingens, Dan Phaneuf, Edson Severnini, and Nicolas Ziebarth, as well as the participants at the 2022 Essen Health Conference; the 2023 Harvard Climate Economics Pipeline Workshop, the 2024 Maastricht Workshop on Applied Economics of the Environment (MAEE), the 2024 Mannheim Conference on Energy and the Environment (MCEE), the 2025 Conferences of the European Association of Environmental and Resource Economists (EAERE), the 2025 Conference of the Association of Environmental and Resource Economists (AERE); the 2023 Learning and Work Seminar at Maastricht University, and the 2024 IHS Talk at the Institute for Advanced Studies in Vienna for valuable feedback and suggestions.

1 Introduction

Rising global temperatures and the increasing frequency of extreme heat events, driven by anthropogenic climate change, are expected to have significant negative consequences for labor markets worldwide (Deschenes 2011). Extreme temperatures can impair physical comfort and cognitive functioning, raising concerns that growing heat exposure may reduce labor supply (Graff Zivin and Neidell 2014). While a growing body of research documents the health impacts of heat, particularly among vulnerable populations such as the elderly (e.g., Carleton et al. 2022, Heutel et al. 2021, Barreca et al. 2016, Deschênes and Greenstone 2011) and children (e.g., Isen et al. 2017a, Graff Zivin et al. 2018, Park et al. 2020), much less is known about its direct effects on the working-age population's capacity to engage in and sustain work. Existing evidence is often limited to specific occupational groups, such as agricultural or outdoor workers (Flouris et al. 2024), or to rather severe outcomes, such as workplace injuries (Dillender 2021, Park et al. 2021, Drescher and Janzen 2025) and mortality (Wilson et al. 2024), which, while important, leave broader impacts on labor market performance insufficiently understood.

A broader understanding of the labor market consequences of heat is essential for at least two reasons. First, the cumulative economic costs of heat-related work disruptions can be substantial. Absences due to heat can interrupt workflows, reduce productivity, and increase strain on remaining staff. These disruptions can translate into significant economic losses, both in terms of forgone labor supply and lost earnings for workers, as well as increased expenditures for employers and insurance systems. Second, heat exposure is unevenly distributed across occupations, with certain groups facing much higher risks. More exposed workers are disproportionately represented in outdoor occupations and jobs with hazardous conditions and limited adaptive capacity. Yet, indoor workers are not exempt from risk: those in poorly ventilated settings or without access to air con-

 $^{^1} For instance,$ in Germany, where universal access to paid sick leave is guaranteed, expenditures related to work absences account for roughly 4% of gross national income (BAuA 2022).

ditioning, as well as older employees with underlying health conditions, may also experience considerable heat stress. A comprehensive assessment of heat's labor market effects must therefore account for its impact across the full spectrum of working environments and demographic groups.

This paper investigates how prolonged exposure to heat influences sick leave among the German working-age population, both in the short and long term, and examines how these effects vary across the labor force. We link high-frequency administrative health insurance microdata covering approximately one-third of the German workforce with quasi-random variation in the occurrence of heat waves at the zip code-by-day level over more than a decade. This allows us to characterize how sick leave responds to varying intensities and durations of heat exposure. The rich detail in the health insurance data enables us to examine heterogeneity in heat-related effects both across individual-level morbidity profiles, and occupational characteristics. By analyzing workers across the full range of occupations, not just those in outdoor or high-risk jobs, and by considering a broad spectrum of health-related absences beyond workplace injuries, we offer the first comprehensive assessment of the workforce's vulnerability to heat waves. This approach can holistically inform adaptation and occupational health measures. Moreover, in leveraging complete histories of claimed healthcare services, we move beyond short-term responses to identify persistent declines in labor supply and sustained increases in expenditures for healthcare utilization in the longer-term.

The German context provides an ideal setting for this analysis. Health insurance coverage is mandatory, and all workers are entitled to statutory sick leave, which protects them against temporary income losses due to illness-related absences. Due to strict reporting requirements, health insurance funds maintain comprehensive administrative records on sick leave, allowing for detailed and population-wide analysis. Our study utilizes data from AOK, Germany's largest public health insurer, drawing on a sample of approximately 9.7 million working individuals aged 25 to 59 over the period 2007 to 2020. Compared to other

commonly used health outcomes, such as mortality or hospitalization, sick leave captures a broader range of health impairments, including milder or non-acute conditions that do not result in death or emergency care but still affect the ability to work. This allows for the identification of more subtle health effects at the individual level, which can accumulate to substantial damages when aggregated across the labor force.

We structure our analysis in three parts. First, we estimate the average causal effect of heat on sick leave using a two-way fixed effects model that exploits quasi-random variation in the daily occurrence of high temperatures within zip code areas over more than a decade. In addition to the standard binary indicator for extreme heat, in the spirit of Miller et al. (2021), we base treatment on the duration and intensity of heat exposure, which characterize a heat wave. This accounts for the fact that the working population is generally less vulnerable than the elderly or children. Prime-age workers may only react to heat under prolonged and intense exposure, which significantly increases discomfort and health risks (Anderson and Bell 2011, D'Ippoliti et al. 2010). Second, we examine heterogeneity in treatment effects using a machine learning-based inference approach proposed by Chernozhukov et al. (2018). We train a gradient-boosted decision tree on an extensive set of over 360 variables, including demographic characteristics, health histories, occupational information, local environmental conditions, and fixed effects, to predict each worker's daily heat-absence risk. Based on these predictions, we stratify workers into distinct ex-anterisk groups and estimate the causal effect of heat exposure on sick leave within each group. Third, we leverage the longitudinal structure of our administrative health records to examine the monetized longer-term effects of severe heat waves, defined as at least three consecutive days with temperatures of 30°C or higher. To this end, we conduct event study analyses that identify changes in expenditures linked to sick leave and medical treatments by a doctor in the years following exposure.

We produce three key findings. First, heat increases sick leave among workers in the short run. On an average hot day, the number of new sick leave cases increases by about 3.5%. This short-term effect grows in magnitude with the duration of exposure. On the third day of consecutive heat stress, the effect increases to 5.0%, and it roughly triples to 10.8% after seven consecutive heat days. We find that heat-related increases in sick leave are driven by a range of disease groups, extending beyond the expected ones such as cardiovascular conditions. This suggests that heat may not only trigger new health issues but also exacerbate existing conditions, thereby pushing individuals at the margin of work capacity into sick leave.

Second, the short-term effects of prolonged heat exposure on labor supply distribute highly unevenly across workers. On the third day of consecutive heat exposure, we observe that the increase in sick leave cases is more than 8.5 times higher among the top 1% of workers at highest predicted heat-absence risk compared to the bottom 50% of the risk distribution. Workers in the higher-risk group tend to be older, the share of male workers is higher, and chronic diseases, ranging from adiposity, over high blood pressure, to chronic respiratory diseases, are more prevalent. Controlling for these individual demographic and health characteristics, we categorize workers into 36 occupational groups and find that those with the highest heat-absence risk are more commonly employed in the transport and logistics, manufacturing, agriculture, and construction sectors. In contrast, lower-risk workers are more prevalent in information technology, education, law and administration, and financial services. Common occupational characteristics of high-risk workers are more physically demanding tasks, a higher exposure to extreme temperatures and outdoor conditions, and a lower income. They are less free to schedule and adjust their working hours and their satisfaction with their job is lower. This finding underscores that heat disproportionately affects the already disadvantaged segments of the workforce.

While the heat-absence risk distributes unevenly across occupations, a key finding of our study is that a three-day heat wave increases sick leave cases across all occupation groups, even among those least affected. This highlights that focusing ex-ante only on those assumed to be high-risk leads to underestimation.

Back-of-the-envelope calculations suggest that a three-day heat wave covering Germany results in income compensation costs from heat-induced sick leave of about 32 million € across occupations. This estimate is a conservative lower bound of the total short-term effects of heat on labor supply, neglecting, e.g., the lower productivity of co-workers who are at work, disruptions to downstream industries, and ripple effects across occupations. For instance, for the health sector, we estimate 24,680 additional absence days by medical professionals from a three-day heat wave. These absences are likely to lead to treatment and service shortages that could affect other workers and amplify costs through supply-side constraints.

Third, heat waves lasting at least three days lead to sustained increases in expenditures for sick leave and doctor visits in the four years following exposure. On average, a three-day heat wave results in persistent cost increases of 2,715 c for sick leave and 124 c for doctor visits per 1,000 workers and quarter. Suggestive evidence implies that the sustained cost increases arise through at least two extensive margin channels: (a) heat waves can trigger new, incisive health shocks with long-lasting impairments of workers' health and ability to work, such as strokes; (b) by temporally exacerbating symptoms that prompt individuals to seek medical attention, heat waves may lead to the formal diagnosis of diseases that likely existed before, such as depressive disorders. Once diagnosed, these previously untreated conditions may result in persistent treatments and recurring work absences. Heat episodes may, thus, play a role in revealing latent disease burdens, which is important for putting the magnitude of the long-term effects into perspective.

This paper makes several original contributions. Most notably, it offers comprehensive new evidence on the occupation-specific channels through which heat exposure affects labor market outcomes. While a large body of research has documented the detrimental impact of high temperatures on human health (e.g., Carleton et al. 2022, Karlsson and Ziebarth 2018, Barreca et al. 2016, Deschênes and Greenstone 2011, Wilson et al. 2024), and a growing number of studies have

shown that heat reduces economic productivity and income (e.g., Zhang et al. 2018, Behrer and Park 2017, Deryugina and Hsiang 2014, Deschênes and Greenstone 2007), far less is known about how heat-induced health impairments translate into reduced labor supply and how these effects differ across occupational groups. The link between environmental health shocks and individual work capacity has only recently begun to receive attention. For example, Graff Zivin and Neidell (2014) use the American Time Use Survey and LoPalo (2023) data from the Demographic and Health Surveys Program to estimate heat-related reductions in labor supply, while Dillender (2021), Park et al. (2021), Ireland et al. (2023), and Drescher and Janzen (2025) examine heat effects on workplace injuries and illness compensation claims in the US, Australia, and Switzerland, respectively. Outside of the economics literature, research has largely focused on heat impacts in specific occupational groups considered especially vulnerable due to outdoor exposure and physical exertion, such as postal and delivery workers, vineyard laborers, military personnel, and athletes, who are often relatively young and healthy (Ioannou et al. 2017, Tannis 2020, Grimbuhler and Viel 2021, Flouris et al. 2024). To the best of our knowledge, this paper is the first to use administrative microdata on sick leave to comprehensively assess how heat exposure affects the ability to work across the general labor force.²

Another distinctive feature of this study is that it goes beyond estimating shortterm responses by tracking the persistence of heat-related health effects over time. Leveraging the longitudinal structure of administrative health records, we conduct event study analyses to identify not only the immediate impact of severe heat waves on sick leave but also delayed and lasting effects on work absences and broader healthcare utilization. This allows us to capture sustained health impairments, such as lingering illness or exacerbation of chronic conditions that may not be reflected in immediate sick leave spikes but still carry important labor market and welfare implications. By documenting these longer-term impacts, we contribute new evidence on the cumulative burden of heat exposure on workers'

²For related work using sick leave data in the context of air pollution, see Holub et al. (2020).

health and labor supply. To the best of our knowledge, the persistence of health and labor market effects from heat shocks among the adult working population have not been studied before. In a paper most closely related to ours, Isen et al. (2017a) show that prenatal exposure to heat days is associated with a reduction in adult earnings at age 30. While this provides first evidence for lasting impacts of heat, they stem from in-utero exposure, which is a particularly vulnerable phase of development (Almond and Currie 2011). Our evidence for long-term increases in work absence and morbidity also adds to an emerging literature on the persistence of adverse effects from other environmental hazards, such as air pollution (Sanders 2012, Isen et al. 2017b, Simeonova et al. 2019, Klauber et al. 2024, Colmer and Voorheis 2025).

Finally, our setting with comprehensive health microdata offers a unique context for characterizing the occupation-specific heterogeneity in how heat-induced health damages materialize in decreased labor supply, and its distributional implications. By leveraging this unusually rich data within a flexible machine learning framework for estimating heterogeneous treatment effects, as proposed by Chernozhukov et al. (2018), we aim to uncover more nuanced causal relationships. This contributes to a growing literature that builds on similar approaches to model complex, high-dimensional interactions between covariates that may jointly influence effect heterogeneity in diverse contexts examining academic tutoring, health programs, fintech adoption, and air pollution among others (Guryan et al. 2023, Bhat et al. 2022, Breza et al. 2020, Deryugina et al. 2019). By showing the highly unequal impacts across occupations that correlate with already existing labor market inequalities, we also contribute to a broader labor economics literature that focuses on exacerbating labor market inequalities induced by other shocks, such as technological progress, automation and artificial intelligence (Acemoglu 2002, Acemoglu and Restrepo 2018, Acemoglu 2024).

2 Data

2.1 Institutional Background

The German welfare system provides universal statutory sick leave to protect workers against temporary income losses arising from workplace absences due to illness (see Swart et al. 2014). From the first day of illness, workers receive 100% of foregone gross wages from their employers for the first six weeks of absence. Afterwards, the public health insurance takes over and provides compensation payment that usually equals 70% of the gross salary, but at maximum 90% of the net income. On an average working day in 2021, approximately 4.34% of employees in Germany were absent from work due to illness (BMG 2022). The resultant expenditures amount to roughly 4% of the gross national income (BAuA 2022). Hence, the costs associated with sickness absence, both in terms of forgone labor supply and economic costs, are substantial.

Strict reporting regulations apply for sick leave. As soon as a worker falls sick, she is obliged to inform her employer immediately of the expected duration of her absence. Cases of absence lasting more than three calendar days must be certified by a physician who issues a certificate attesting the incapacity to work ("Arbeitsunfähigkeitsbescheinigung").³ However, the employer may request the certification earlier. By law, the certificate of work incapacity must be sent not only to the employer, but also the health insurance fund without delay (EFZG, § 5). It is the responsibility of the worker to do so. They have incentives to adhere to this rule because they otherwise risk losing their entitlement to continued payment of wages in the event of longer-lasting illnesses. Accordingly, health insurance funds are able to register about 95% of the total sick leave rate (Marschall et al. 2017). The cases of sick leave that they do not capture are mostly those of short duration lasting less than three days or instances where workers fail to fulfill their obligation to report their absence to the health insur-

³A person is incapacitated for work if she is no longer able to perform the tasks that she recently performed, or is only able to perform them at the risk of aggravating the illness (§ 92 Abs. 1 Satz 2 Nr. 7 SGB V).

ance fund. We assume that behavioral factors, such as shirking, are more likely to influence these shorter cases, as workers can avoid the burden of visiting a physician and undergoing a medical examination. In contrast, cases recorded by health insurance are more likely to reflect genuine, health-related work absences, representing a lower bound for the full extent of sick leave.

Based on this regulatory framework, health insurance funds have comprehensive and detailed administrative information on sick leave for the German population. In particular, they receive precise information on the medical reason for each case of sick leave on the submitted medical certificate. For privacy reasons, this information is not submitted to the employers.

2.2 Sick leave and morbidity data

We obtain sick leave data from Germany's largest public health insurer AOK. Of the roughly 90% of the German population that is publicly insured⁴, AOK covers about a third. This comprehensive coverage ensures that individuals from all population subgroups are represented (Jaunzeme et al. 2013). The "AOK Research Institute" provides us with pseudonomized data at the level of the individual for all workers aged 25 to 59. This "prime age" group comprises individuals with a regular employment contract, but also self-employed individuals and freelancers who decided against private insurance. Overall, the data comprise about 9.7 million workers, which we observe over a 14-year period from 2007 to 2020.

The daily sick leave data we obtained is based on the medical certificates issued by physicians. It holds information on the start and end date of each sick leave case as well as its medical reason classified according to the ICD-10 system.⁵ We combine this data with information on the insured individuals, i.e., their sex, birth date, location of residence at the 5-digit zip code level, and occupation

⁴The remaining 10%, in particular civil servants, self-employed, and high-income workers, are insured privately.

⁵The ICD-10-Code is an international system for the statistical classification of diseases and related health problems provided by the WHO. Germany uses the extended version ICD-10-GM (DIMDI n.d.).

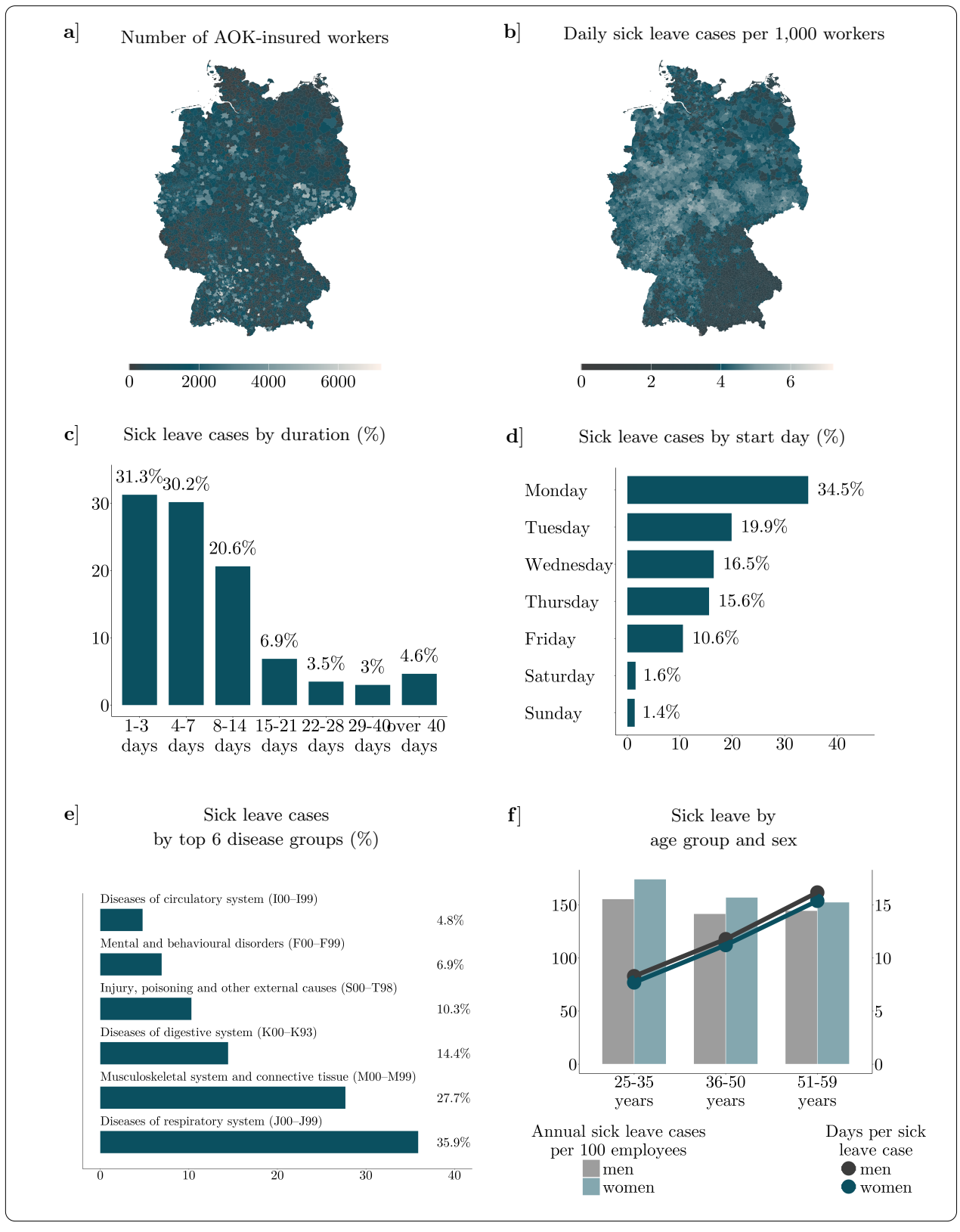
group. Occupations are categorized according to the German Classification of Occupations (KldB-2010), which aligns closely with the International Standard Classification of Occupations (ISCO-08).⁶

Figure 1 provides a descriptive overview of the sick leave data. On average, a zip code area covers 856 insured individuals, but there are regional differences (Panel a). The number of sick leave cases per 1,000 workers is highest in the northwestern part of Germany and lowest in the southeastern region of Bavaria (Panel b). Sick leave spells differ in length (Panel c). About 30% of all cases last only one to three days, another 30% last less than a week, and about 5% of all cases cause long-term absences that last 40 days or more. The day of the week is a strong predictor for the number of individuals that call in sick. About 35% of all cases begin on a Monday while only few cases start on a Saturday or Sunday (Panel d). This is because workers who fall ill on the weekend can usually get a sick note only on Monday when the doctors' offices are open. Panel e) presents the six disease groups that are most often reported on sick leave certificates. About 36% of all cases are linked to respiratory diseases, followed by 28% linked to problems of the musculoskeletal system and the connective tissues, and 14% linked to issues of the digestive system. Across all age groups, women call in sick more often than men (Panel f). While the duration of sick leave increases with age for both sexes, men are on sick leave slightly longer than women, on average. In Appendix Table A.1, we provide additional descriptives.

_

⁶In 2011, the KldB-2010 system replaced the older KldB-1988/92-system. To ensure comparability of the occupation data throughout our period of observation, we map the data in the years before 2011 into the newer KldB-2010 scheme. Additionally, we observe the economic sectors of jobs, classified according to the German Classification of Industries (Klassifikation der Wirtschaftszweige, WZ 2008), which is based on the Statistical Classification of Economic Activities in the European Community (NACE, Revision 2), which we incorporate into our heterogeneity analysis.

Figure 1: Descriptive statistics on sick leave



This figure provides a descriptive overview of the sick leave data. The maps show the number of AOK-insured workers per zip area in Panel a) and the daily number of sick leave cases per 1,000 AOK-insured workers in Panel b). The barplot in Panel c) illustrates the percentage share of all sick leave cases that last for the number of days specified on the x-axis. Panel d) presents the percentage share of all sick leave cases that start on the weekday specified on the y-axis. In Panel e), we plot the percentage share of sick leave that is due to the six disease groups that most often cause absence from work. In Panel f), we illustrate differences in sick leave by age group and sex. The y-axis measures the annual number of sick leave cases per 100 workers on the left-hand side and the average duration of these cases in days on the right-hand side.

In addition to the daily sick leave data, the AOK Research Institute provides quarterly data on morbidity based on healthcare utilization patterns on a rolling basis. For every worker, we observe the average quarterly number of outpatient treatments by a doctor measured over the previous eight quarters. In addition, we also obtain 58 quarterly binary indicators identifying the presence of specific chronic diseases. The indicators capture, for instance, whether workers suffered from cancer, diabetes, adiposity, cerebrovascular disease, affective disorders, and respiratory diseases, in the previous eight quarters. A full overview is available in Appendix Table A.2. All morbidity variables are available for workers continuously insured during the preceding eight quarters, starting from 2008. However, because the morbidity variables are measured over a moving eight-quarter time window, the exact timing of the recorded treatments and diagnoses within that period is unknown.

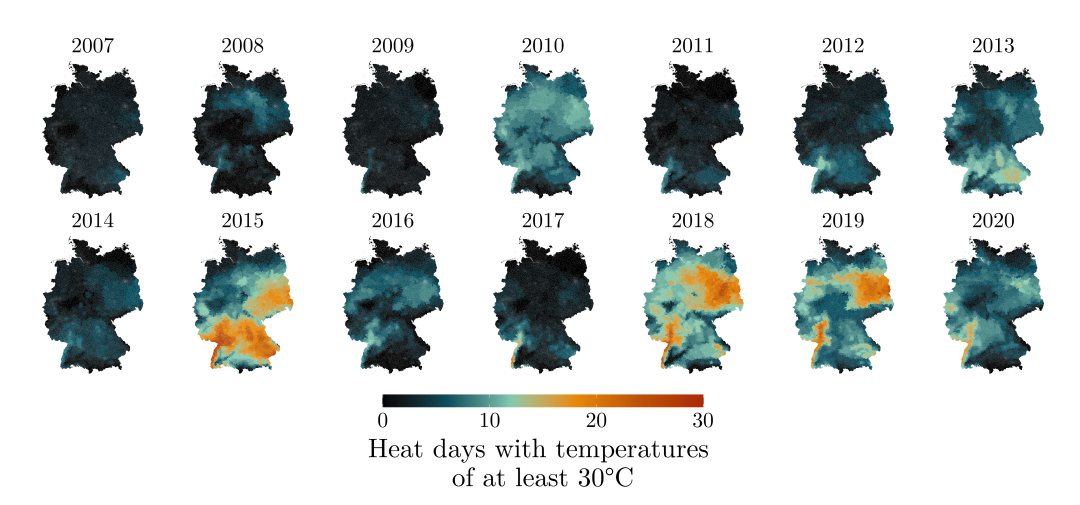
2.3 Weather data

The European Center for Medium-Range Weather Forecasts (ECMWF) provides meteorological data. We use the ERA5 land product for the years 2007 through 2020, which divides the surface of the Earth into a grid with a latitude-longitude resolution of approximately $0.1^{\circ} \times 0.1^{\circ}$ and provides hourly data for each grid cell.⁷ For every day and grid cell, we extract the maximum and minimum temperature measured two meters above the ground, the total amount of precipitation, relative humidity, and wind speed. Based on the daily maximum temperature, we calculate a heat day indicator which is equal to one, if temperatures are 30°C or higher. To aggregate the weather data to the level of zip code areas, we take the weighted sum of the amount of precipitation and the weighted averages of all other variables, with weights equal to the population size in each grid cell.⁸ Heat days at the zip code level are defined as days when the aggregated heat

⁷There are a few grid cells in Germany that the ERA5 land product does not cover. For these cells, we use ERA5 data with a lower resolution $(0.25^{\circ} \times 0.25^{\circ})$.

 $^{^{8}}$ We use raster data for the working-age population with a 100-meter resolution from WorldPop Hub (2018).

Figure 2: Geographic variation of heat in Germany from 2007 to 2020



indicator is greater than zero. Figure 2 illustrates the variation in the occurrence of heat across Germany and the 14 years of our observation period.

We construct several alternative measures of heat exposure. First, we define variables that capture the duration, i.e., number of consecutive heat days, and the intensity of exposure, i.e., the temperature in degree Celsius above 30. Additionally, we construct our heat day indicator using apparent temperatures rather than maximum temperatures. To this end, we calculate the perceived temperature derived from either a combination of temperature and wind speed or temperature and humidity, according to the definition by the US National Weather Service (NWS 2024a, NWS 2024b). Moreover, we define an indicator variable for tropical nights, which is equal to one if the minimum temperature does not fall below 20°C. Summary statistics for these exposure measures are available in Appendix Table A.4.

2.4 Occupational data and additional covariates

We obtain additional data on working conditions by occupation from the Federal Institute for Vocational Education and Training. It is based on representative survey data that describe the skill requirements and working conditions linked to different professions in Germany (Gensicke and Tschersich 2018). The data

is collected every six years from around 20,000 employed individuals. From the 2018-survey wave, we extract data that capture to what extent employees (i) work under very high and very low temperatures, (ii) work outdoors, (iii) perform physically demanding tasks, (iv) are free to schedule and adjust their working hours, and (v) are satisfied with their job. Table A.5 in the Appendix shows the survey questions that we match to each of these five dimensions. If there is more than one relevant question, we summarize the information from the different questions in an index based on principal component analysis. In addition, we consult data from the Federal Employment Agency on (vi) the median income in each occupation group (Federal Employment Agency 2021).

Lastly, we compile a host of almost 300 mostly time-invariant variables from diverse sources to characterize workers' places of residence. These variables capture demographic factors (e.g. age distribution, share of foreigners, and average household size), socioeconomic characteristics (e.g. share of households in different socioeconomic status classes, and availability of social service facilities), and infrastructure (e.g. number of outpatient medical practices, available greenspace area, and age of buildings). We derive these zip-code-level variables from raster data in the 2011 Census provided by the Federal and State Statistical Offices, geodata from OpenStreetMap, and commercial data from Acxiom. Appendix Table A.3 offers a summary overview of the captured zip code characteristics.

3 Methodology

3.1 Identifying short-term effects of heat exposure

In the first part of our analysis, we aggregate individual sick leave data by zip code area and day, separately for sex (male vs. female) and age groups (25–35, 36–50, and 51–59). Based on the aggregated data we run a two-way fixed effects model to estimate the effect of an average single heat day on sick leave

⁹Acxiom is a service provider specialized in spatial customer and business information for marketing.

$$S_{zdy}^{ag} = \beta H_{zdy} + \delta_1 P_{zdy} + \delta_2 F_{syd} + \gamma_{zm} + \gamma_{wy} + \gamma_{km} + \gamma_d + \gamma_a + \gamma_g + \epsilon_{zdy}^{ag} \quad (1)$$

where the dependent variable S_{zdy}^{ag} is the number of sick leave cases that are newly reported on day d in year y per 1,000 workers living in zip code area z and belonging to age group a and sex group g.¹⁰ If the daily maximum temperature in a zip area reaches at least 30°C, the binary indicator H_{zdy} equals one, otherwise it is zero. Our coefficient of interest, β , provides an estimate of the average effect of a day with temperatures of at least 30°C on sick leave.

We control for zip code level precipitation on the same day, P_{zdy} , as well as public holidays, F_{sdy} , that vary by day and state s. Zip code by calendar month fixed effects γ_{zm} control for unobserved time-invariant determinants of sick leave by zip code, as well as zip code specific seasonal differences across months (e.g. the spreading of influenza or the number of seasonal workers). Week by year fixed effects are captured by γ_{wy} and account for country-wide economic shocks and trends common to all workers. Because sick leaves follow strong within-week patterns (see Figure 1), we add day-of-the-week fixed effects γ_k that account for patterns in sick leave tied to the day of the week k. In our preferred specification, we allow them to vary across calendar months to address that the amount of weekend work is dependent on the season in some professions (e.g. in tourism, hospitality, and event management). Moreover, we add dayof-the-year fixed effects γ_d to pick up seasonal fluctuations in sick leave within months. Lastly, we absorb differences in sick leave common to each age and sex group, by including γ_a and γ_g , respectively. All regressions are weighted by the number of workers in a zip-age-sex cell. We cluster standard errors at the county level.

 $^{^{10} \}rm When$ constructing this variable, we exclude those workers who are already on sick leave on day d from the denominator.

¹¹For example, they capture that heat days occurring on a weekend are unlikely to result in new sick leave cases because most physicians are available only during the week.

In addition to the standard binary indicator for heat exposure H_{zdy} , we adapt Equation 1 and base treatment on the duration and intensity of heat exposure, which characterize a heat wave. This accounts for the fact that the working population is generally less vulnerable than the elderly or children and may only react to heat under prolonged and intense exposure. To this end, we replace βH_{zdy} with $\sum_{\tau=0}^{9} \theta_{\tau} E_{zdy}^{\tau}$, where E_{zdy} measures either the duration or the intensity of exposure. We bin the exposure variables in τ intervals. For exposure duration, the first bin equals one if day d in year y and zip area z corresponds to the first day with at least 30°C in a row, the second bin equals one if it is the second day with heat in a row, and so forth. For exposure intensity, we bin temperatures of at least 30°C into 0.5-degree bins.

Our analysis rests on three assumptions. First, conditional on the fixed effects and control variables included in our model, we assume the occurrence of heat days to be quasi-randomly distributed. Second, we assume that heat exposure which we assign to workers based on their zip code of residence, reflects their actual exposure reasonably well. While we cannot observe the workers' workplace locations, we expect that, except for few individuals who commute very long distances, heat exposure at home is likely highly correlated with exposure at work. However, it is not even clear to what extent exposure at work and at home drive sick leave. Both high temperatures during work and the lack of recovery periods during leisure time and night at home may play a role. We consider our treatment assignment a reasonable proxy for the more complex concept of heat exposure.

Third, we assume that the start of sick leave aligns with the occurrence of heat exposure. However, since workers may provide a medical certificate up to three days after falling ill (see Section 2.1), there may be delays in reporting. It is unclear to what extent this delay occurs. In principle, workers shall consult a physician immediately, and, even if physicians examine workers a few days after

¹²In 2020, the average commuter distance was 24 km in Germany (Brixy and Haas 2025). While commuting between zip code areas is fairly common, only 15.9% of workers are employed outside their home county, which is the level at which we cluster standard errors, and most of these work in a directly adjacent county (Krause and Kripfganz 2025).

they have turned sick, they may note down the starting date of the sickness retroactively. However, reporting delays are likely to exist and could lead to underestimating the heat effects. To test for this we re-estimate Equation 1 while allowing for effects that occur with a lag of up to three days post treatment.

To implement our regression analysis, we have to address computational limitations. Due to the large data size, we construct a smaller dataset by retaining all heat-exposed observations and adding a randomly sampled control group of approximately 10 million observations. This yields a final sample of about 13.3 million zip-age-sex-year-day-level observations.¹³

3.2 Machine Learning inference on heterogeneous heat effects

To identify effect heterogeneity in the second part of our analysis, we return to the non-aggregated data at the level of the individual worker and implement a machine learning based inference approach proposed by Chernozhukov et al. (2018).

First, we randomly split all worker-day observations into two datasets, the training and main datasets, each covering a mutually distinct subset of about 50% of all workers. In the training dataset, we assign all worker-day observations with exposure to at least 30°C to the treatment and the rest to the control group, and train a prediction model using a gradient tree boosting algorithm for each group. Both models forecast sick leave cases, S_{izdy} , for worker i living in zip area z on day d in year y based on the covariates Z_{izdy} . The covariates include detailed information about the insured workers, such as their exact age, sex, health status, and occupation (classified according to the three-digit KldB-2010 code). They also include daily precipitation levels and characteristics of the workers' zip code area of residence, capturing population demographics, socioeconomic

¹³With 8,174 zip code areas, three age groups, two sexes, and 5,114 days, our full sample covers about 250 million observations. The data size prevents us from running a single regression on the full sample. In addition, the probability of heat exposure on any given day is relatively low. Therefore, we run regressions on a subset of the control observations in our data, ensuring that the sample is sufficiently large to preserve the robustness of our findings.

¹⁴We use the open-source distributed gradient-boosting framework LightGBM developed by Microsoft.

status, and the number of outpatient medical practices, for instance. We provide an overview of our binary variables capturing workers' morbidity status in Appendix Table A.2 and summarize the dimensions captured by our residential zip code variables in Table A.3. Although the covariates come with varying temporal and spatial resolution, we collectively index them at the worker-day level, izdy, for ease of notation. Additionally, Z_{izdy} includes county, year, month, and day-of-the-week fixed effects. Next to the two models predicting sick leave cases for the treatment and control group, we train a third model that rests on all worker-day observations in the train data set and predicts the propensity score, i.e., heat exposure H_{zdy} as a function of the covariates Z_{izdy} .

Second, we predict the probability of a sick leave case for each worker-day in the main data set using the models trained for the treatment and control group. This yields two predicted probabilities: one assuming that worker i is exposed to heat on day dy and the other assuming she is not. The difference between both predictions, $\hat{V}(Z_{izdy})$, corresponds to the sick leave probability attributable to heat. It serves as a proxy for the individual's risk of daily heat-absence. Additionally, we predict the propensity score $\hat{p}(Z_{izdy})$ for each worker-day. Based on the main data we estimate the following weighted regression to obtain Sorted Group Average Treatment Effects (GATES):

$$S_{izdy} = \alpha + \sum_{l=1}^{6} \lambda_l (H_{zdy} - \hat{p}(Z_{izdy})) \cdot 1(G_l) + \theta \hat{S}^C(Z_{izdy}) + \epsilon_{izdy}, \qquad (2)$$

where the weights equal

$$w(Z_{izdy}) = \frac{1}{\hat{p}(Z_{izdy})(1 - \hat{p}(Z_{izdy}))}.$$

¹⁵Individual information are registered quarterly, precipitations comes at the zip area-day level, and characteristics of the place of residence are time-invariant and available at the zip area level (see Section 2.4).

¹⁶The gradient tree boosting algorithm accommodates interactions among all variables and fixed effects.

The indicator $1(G_l)$ is equal to one if the predicted heat-absence proxy, $\hat{V}(Z_{idy})$, of worker i on day dy belongs to group l. To define groups, we split the proxy values into increasingly small intervals, with the 0th, 50th, 75th, 90th, 95th, and 99th percentiles as lower interval bounds. The coefficients λ_l represent the average heat effects on sick leave cases for these groups of varying predicted heat-absence risk. To explore how effects change by the day of exposure duration, we estimate Equation 2 separately, allowing H_{zdy} to represent the first through ninth consecutive day of heat sequentially. For greater precision, the model also includes the predicted sick leave probability for days with no heat $\hat{S}^{C}(Z_{izdy})$.

We examine the characteristics of workers who are differently affected by heat exposure using Classification Analysis (CLAN). To this end, we examine the prevalence of individual characteristics, pre-conditions, and workplace characteristics in the group of workers belonging to the top 10% with the highest predicted heat-absence risk values, $\hat{V}(Z_{idy})$, in comparison to those belonging to the bottom 50% with the lowest values, respectively. We, first, compare the sex and age of the workers in both groups. Then, we test for statistical differences concerning the existence of several chronic diseases, while controlling for age and sex. And, finally, we explore differences across 36 occupation groups (defined by the two-digit occupation code) and six workplace characteristics (i.e. exposure to extreme temperatures, outdoor work, physical demands, job flexibility, worker satisfaction, and median income), while controlling for the effects of sex, age, and morbidity.

To address computational challenges posed by the large individual-level dataset, we limit the ML-based heterogeneity analysis to the summer months May through September, ¹⁷ apply a downsampling-strategy, and run regressions on 250 data partitions. Appendix Section C provides a detailed description of our implementation approach.

¹⁷As a robustness check, we also restrict our sample for estimating Equation 1 to the summer months. Appendix Table A.10 shows that the results remain robust.

3.3 Identifying long-term effects of heat exposure

In the third part of our analysis, we estimate long-term effects of extreme heat events on the costs for sick leave and other healthcare services in the years after exposure. To this end, we restrict our sample to workers who are consistently insured and employed, while also residing in the same zip code area throughout the study period. This allows us to ensure a balanced sample for which we can accurately track exposure to extreme heat over time. We aggregate these observations at the zip code by quarter level, stratified by gender and across the G_l groups of varying heat-absence risk identified in Section 3.2. ¹⁸ As a result of enforcing a balanced sample, our sample size is reduced significantly to 3,244,386 observations. We focus our analysis on heat events that persist for at least three consecutive days, and estimate the following event-study model:

$$Y_{zqy}^{gl} = \sum_{t=-3}^{4} \theta_t Wave_{zqy}^t + \delta_1 P_{zqy} + \gamma_{zy} + \gamma_{sqy} + \gamma_g + \epsilon_{zqy}^{gl}$$
 (3)

where Y_{zqy}^{gl} refers to the expenditures for either (i) income compensation due to sick leave or (ii) the average number of outpatient treatments by a doctor, both measured per 1,000 workers living in zip code area z, belonging to sex group g and risk group l, reported in quarter q in year y. We calculate expenditures based on aggregate statistics. For sick leave, we multiply the number of sick leave days in each quarter with the average median income per day, which is equal to $101.58 \cdot 6.19$ For doctor visits, we multiply the average number of treatments per quarter with $71.11 \cdot 6$, the average cost per treatment in 2020 values (KBV 2019).

¹⁸To ensure that individuals remain in the same risk group over time, we first average their daily predicted heat-absence risk values and then categorize them into percentile groups based on these averages. We do not disaggregate the data by age group, as done in Section 3.1, because age is strongly correlated with the predicted heat-absence proxy that defines the groups G_l .

¹⁹This estimate is based on 2020 data from Federal Employment Agency 2021. We compute a weighted average of the median income across occupational groups, using occupation-specific workforce sizes as weights and adjusting for the proportions of part-time and full-time employment.

²⁰KBV 2019 report a cost of 70.59€ per treatment in Germany (Q4 2019 values; see Table 1), which we adjust for inflation to derive a 2020 value of 71.11€.

 $Wave_{zqy}$ counts the number of heat wave days per zip code area and quarter, and the coefficients θ_t capture the effects of these heat wave days in the years pre and post their occurrence. We bin the endpoints, capturing post-treatment effects that extend beyond the fourth year after treatment and for up to five years prior to heat wave exposure. 21 P_{zqy} captures precipitation. Fixed effects γ_{zy} account for determinants of health care and occupation choices at the zip by year level, e.g. the closure of a factory leading to local employment shocks. In addition, γ_{sqy} absorb quarterly changes at the level of the states, e.g. temporal changes in the healthcare system, which is partially managed at the federal state level. γ_g captures differences in the outcome variable common to each gender.

For interpretation, it is important to note that while both outcome variables vary at the quarterly level, the number of doctor consultations is a quarterly average measured over the previous eight quarters (see Section 2.2). This means that in the initial post-treatment periods, heat wave exposure affects this outcome only partially, which we expect to result in a weaker treatment effect. To somewhat account for this, we weight observations that are only partially exposed to the treatment by the proportion of the treatment duration.²²

We also estimate the treatment effect of heat waves pooled across all posttreatment periods $t \geq 0$. To examine heterogeneity in this effect across workers, we interact the pooled post-treatment indicator with the group indicators for heat-absence risk G_l . In doing so, we focus on the most at risk workers with a predicted heat-absence proxy in the percentiles [90,95), [95,99), and [99,100] and combine the remaining groups into a single, broader category [0,90).

Conditional on the included covariates and fixed effects, we assume strong parallel trends (Callaway et al. 2024), i.e. the path of outcomes for workers in areas with fewer heat wave days reflects that for workers in areas with more heat wave days had they instead experienced fewer heat wave days as well. However, the

 $[\]overline{^{21}}$ To ensure we have data for all t periods for each observation in our study period, we obtain extended weather data ranging from 2003 to 2023.

 $^{^{22}}$ For example, the number of doctor visits is considered untreated in the first quarter post-treatment, treated at 1/8 in the second quarter, at 2/8 in the third quarter and so on. Full treatment is assumed only for outcomes measured after the second year post-treatment.

model does not account for potential bias linked to treatment effect heterogeneity in settings of staggered treatments (Callaway et al. 2024, Athey and Imbens 2022, Goodman-Bacon 2021, de Chaisemartin and d'Haultfoeuille 2020), which we address in our robustness analysis. We cluster standard errors at the county level.

4 Results

4.1 Short-term heat effects on sick leave

We begin by presenting estimates of same-day heat effects on short-term sick leave. Table 1 shows estimates of the effect of an average heat day with at least 30°C on the number of newly reported sick leave cases per 1,000 workers. We find robust heat effects across the different choices of fixed effects, which increase in stringency from left to right. Our preferred specification in Column (3) shows that an average heat day increases cases by 0.152 per 1,000 workers, which equals a relative increase of about 3.5%. Appendix Table A.9 demonstrates that these results remain robust when additionally controlling for state-specific vacation periods.

The same-day effects reported in Table 1 may underestimate the total impact of heat, as some sick leave cases could occur and be registered with a delay. To account for this, in Table A.6 in the Appendix, we gradually include additional days following the heat day. We find that the effects of heat materialize over the day of exposure and the two following days, while we do not find statistically significant changes in sick leave on the third day after exposure. When accounting for these lagged effects, we find that a single heat day results in approximately 0.216 additional cases of absence, equating to about a 5.3%-increase.

The effects vary across different measures of heat exposure. Firstly, Figure 3 shows effect variation by the duration of exposure (i.e. the number of consecutive heat days) and the intensity of exposure (i.e. the average temperature on heat days in degrees Celsius). The effects on sick leave cases increase in mag-

Table 1: Contemporaneous effects of heat days on sick leave

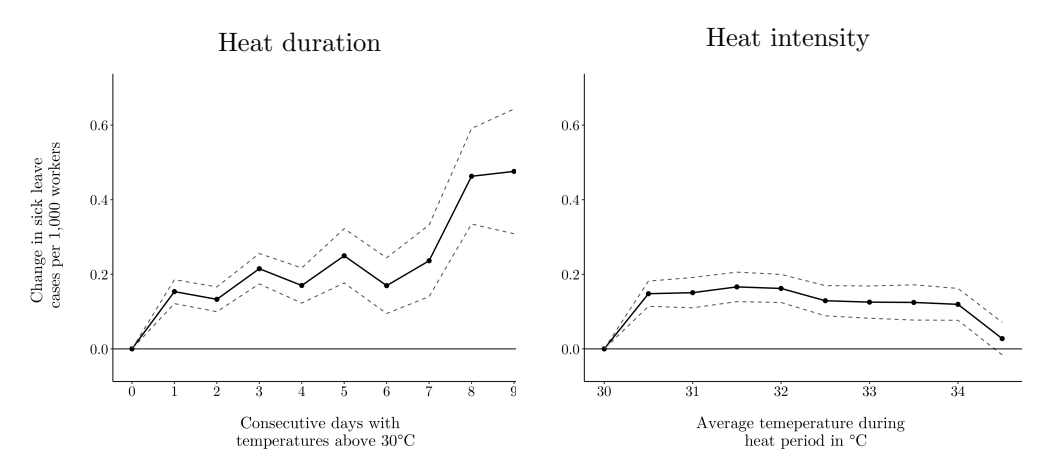
	Sick leave cases per 1,000 workers		
	(1)	(2)	(3)
heat day	0.095***	0.146***	0.152***
s.e.	(0.015)	(0.016)	(0.016)
r.e.	[2.217]	[3.409]	[3.546]
	Fixed effects		
year x week	yes	yes	yes
zip	yes	no	no
day-of-the-week	yes	no	no
zip x month	no	yes	yes
day-of-the-week x month	no	yes	yes
day-of-the-year	no	no	yes

This table reports estimates of the effect of an average heat day on sick leave following Equation (1). Fixed effects become more stringent from column (1) to (3). In (1), we absorb determinants of sick leave specific to the zip area, the week, and the day-of-the-week. To control for seasonal patterns in sick leave, (2) allows the zip area and day-of-the-week fixed effects to vary across calendar months, and (3) adds day-of-the-year fixed effects to also pick up seasonal fluctuations in sick leave within months. The dependent variable refers to new sick leave cases per 1,000 workers. In all regressions, we include controls for age, sex, public holidays, and precipitation. The regressions are weighted by the number of workers per zip-age-gender cell. Standard errors in round parentheses are clustered at the county level. Relative effects in percent are in square parentheses. The sample size is 13, 293, 949 .

* p < .05, ** p < .01, *** p < .001.

nitude with the duration of heat exposure. The effect estimated on the first heat day roughly triples to 0.463 (10.8%) after the seventh day of consecutive heat (numerical estimates are available in Appendix Table A.8). This increase is likely due to a combination of both the lagged impacts of previous heat days and the disproportionate impact of a long exposure duration, which are challenging to isolate empirically. Moreover, heat waves with a length of more than seven days have been rare in Germany, although progressing climate change is increasing their likelihood (Brasseur et al. 2017). Interestingly, we observe no effect differences with increasing intensity of heat in Figure 3. The estimated coefficients follow a flat pattern, suggesting that higher temperatures above 30°C are not necessarily reflected in more sick leave cases. Secondly, we compare how the estimated effects change, when using apparent temperatures of at least 30°C and tropical nights with a minimum temperature of at least 20°C as alternative exposure measures in Appendix Table A.7. We find that the effect of a heat day on sick leave cases increases from 0.152~(3.5%) in column (3) in Table 1 to 0.174(4.1%) when considering apparent instead of regular temperatures to account for the additional burden from relative humidity and low wind flow. However, we observe no effect increase linked to the exposure to tropical nights.

Figure 3: Heat effects by exposure duration and intensity



The figure illustrates how the effects of heat vary by duration (i.e., the number of consecutive heat days) and intensity of exposure (i.e., the average temperature of a heat period). The dependent variable is the number of new sick leave cases per 1,000 workers. The regressions include zip area—month, year—week, day-of-the-week—month, and day-of-the-year fixed effects. We include controls for age, sex, public holidays, and precipitation. The regressions are weighted by the number of workers per zip-age-gender cell. Standard errors are clustered at the county level. Confidence intervals refer to the 5% level of significance.

To shed light on the medical reasons for sick leave on heat days, we use the number of sick leave cases per 1,000 workers by ICD-10 chapter as dependent variables and present the cause-specific effect estimates in Figure 4. We find that high temperatures affect a wide range of diseases. This includes diseases of the circulatory system, injuries and poisoning (which includes damages linked to external causes such as heat and sunlight), mental disorders, and pregnancy- and birth-related complications which several recent studies associate with heat (Park et al. 2021, Banerjee and Maharaj 2020, Mullins and White 2019, Obradovich et al. 2018, Karlsson and Ziebarth 2018, Burke et al. 2018). Also, conditions affecting the musculoskeletal system, such as back pain, and infectious diseases, both common causes of sick leave, increase on hot days. These effects of heat across several disease groups suggest that heat may not only trigger specific health issues that would not otherwise occur, but also exacerbate existing conditions—pushing individuals at the margin to take sick leave. Despite their low absolute frequency, external causes of morbidity and mortality exhibit the highest relative effect (+54.0%). This is a mixed group of sick leave cases, including absences linked to accidents (such as heat-related burns or scalds and

Figure 4: Heat effects on sick leave by disease groups

Disease group $name$	Heat day effect coef. (s.e.) [r.e.]	Additional sick leave cases per 1,000 workers
		Additional sick leave cases per 1,000 workers
External causes Ear diseases Respiratory system	0.000 (0.000) [54.0] 0.000 (0.001) [-0.1] -0.007 (0.004) [-0.6]	· · · · · · · · · · · · · · · · · · ·
respiratory system	0.001 (0.004) [0.0]	-0.01 0.00 0.01 0.02 0.03

This figure reports estimates of the effect of an average heat day by disease group following Equation (1). The dependent variable is the number of new sick leave cases per 1,000 workers for 18 broad disease groups listed on the left. Appendix Table A.11 provides an overview of how the diseases groups are defined in terms of ICD-10 codes. A separate regression is estimated for each disease group. All regressions include zip area—month, year—week, day-of-the-week—month, and day-of-the-year fixed effects. We include controls for age, gender, public holidays, and precipitation. The regressions are weighted by the number of workers per zip-age-gender cell. We report the estimated coefficients in the table and plot them on the right. Standard errors in round parentheses are clustered at the county level, relative effects in percent are in square parentheses. The sample size is 13, 293, 897 . * p < .05, ** p < .01, *** p < .001.

traffic-related injuries), intentional self-harm, assault, and adverse side effects of medical interventions, which, unfortunately, we are unable to disentangle further. We also observe large relative effects for diseases of the circulatory system (+19.8%), followed by skin diseases (+10.7%), and injuries (+8.9%).

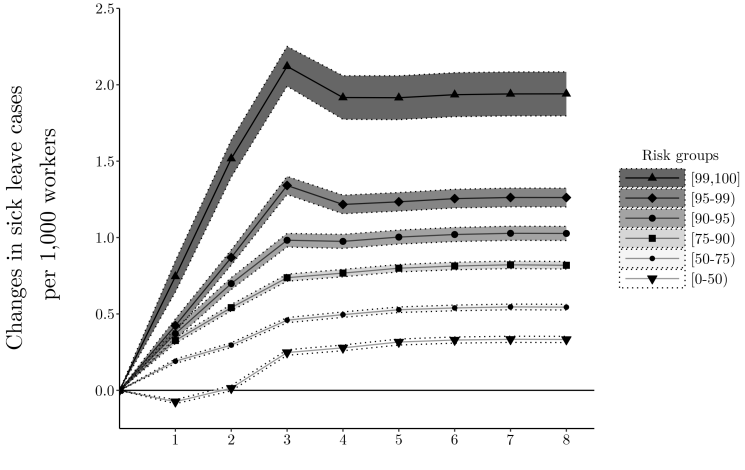
Appendix Figure B.1 shows estimates for cause-specific effects on sick leave by heat duration and heat intensity. While the average estimate across diseases in Figure 3 suggests that effects vary only with the duration of exposure, we now find clear evidence that heat-induced sick leave due to diseases of the circulatory system (I00-I99) are strongly increasing with both the duration and intensity of exposure.

4.2 Heterogeneous heat wave effects on sick leave

Next, we turn to effect heterogeneity by workers' risk of heat-related absence, occupation and working conditions. Figure 5 shows that the effect of heat on sick leave cases increase in a worker's predicted heat-absence risk and as heat exposure persists over days. On the third consecutive day of exposure, effects range from 0.248 in the 50% of workers at lowest risk to 2.121 in the top 1% at highest risk. For all risk groups, effects increase over the first three days and then level off.²³

Table A.12 in the Appendix provides a descriptive comparison between workers in the top decile of the predicted heat-absence risk distribution and those in the bottom half based on a CLAN analysis. Workers in the high-risk group are, on average, 1.56 years older, and the share of male workers is seven percentage points

Figure 5: Sorted Group Average Treatment Effects (GATES) of heat exposure on sick leave cases



Consecutive days with temperatures above 30°C

The figure shows GATES estimates from Equation 2 for workers in predicted heat-absence risk percentiles [0,50), [50,75), [75,90), [90,95), [95,99), and [99,100]. We estimate the heat effect separately by day of exposure duration and report coefficients along with 95% confidence intervals. Standard errors are clustered at the state level. The sample size decreases from 3,445,046,772 on the first to 3,266,872,693 on the ninth heat wave day.

²³While the effects on sick leave are positive for all groups from the second day onward, the lowest-risk group exhibits a small but statistically significant decrease in sick leave on the first day of heat exposure. This pattern may, for instance, result from a higher representation of younger, healthier individuals in this low-risk group, for whom higher temperatures pose

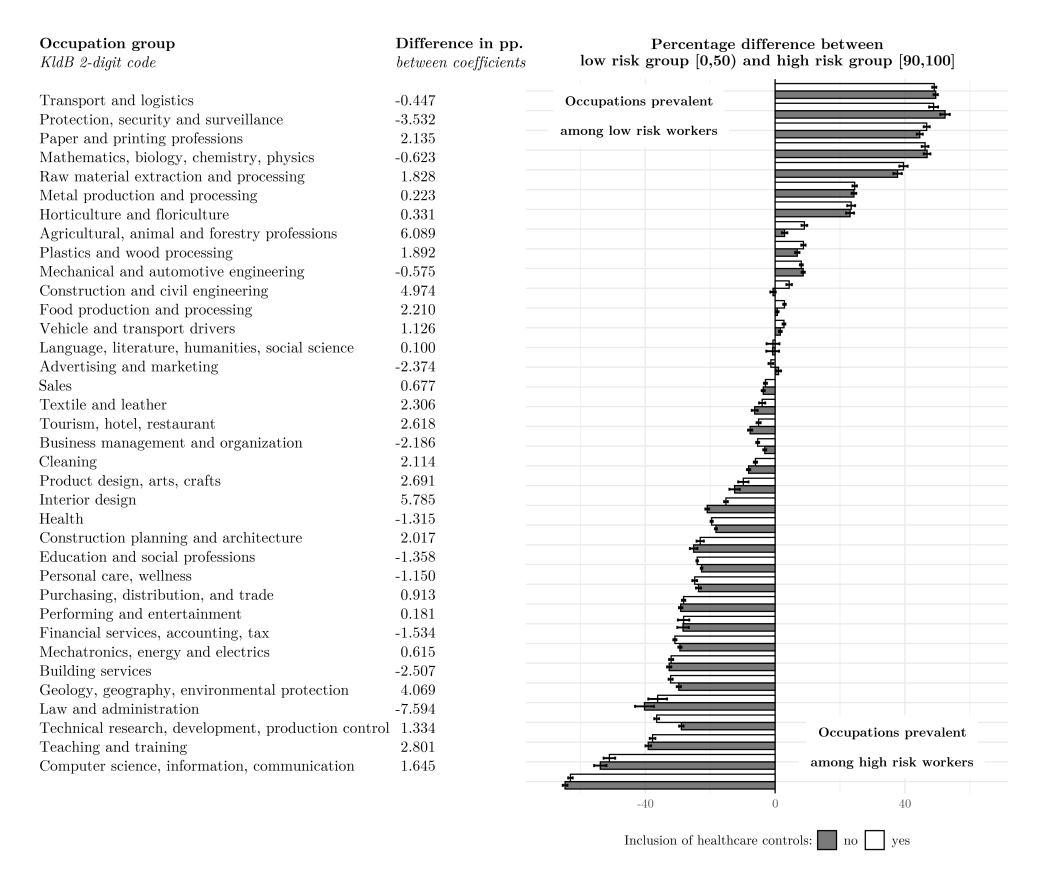
less of a health risk and may even boost motivation and attendance in the short term.

higher. Conditional on age and sex, we find systematic differences in health outcomes between the two groups. High-risk individuals exhibit significantly poorer health: they report 4.08 more doctor visits in the preceding two years and the prevalence of various chronic conditions is higher in the high-risk group. The largest relative differences are observed for cerebrovascular diseases such as stroke (+56.5%), affective disorders such as depression (+48.2%), and cancer (+47.8%).

Next, Figure 6 documents significant heterogeneity of heat-related sick leave across 36 occupations. It illustrates the relative prevalence of each occupation in the high-risk (top 10% of the predicted heat-absence risk distribution) versus low-risk group (bottom 50%). We observe that workers in transport and logistics, manufacturing, agriculture, and construction sectors are more likely to be at risk of heat-related sick leave. In contrast, lower impacts are evident in computer science and information technology, education, law and administration, and in financial services.

A positive differential between the black and white bars in Figure 6 implies that risk attribution increases once individual health characteristics are accounted for. We observe this pattern, for example, in agriculture, construction and civil engineering, as well as interior design. This finding may suggest that the heat-related absence risk associated with greater workplace heat exposure in these occupations is mitigated by lower individual vulnerability; i.e., individuals in these occupations may be relatively young and healthy. Conversely, a negative differential indicates that risk decreases when controlling for morbidity. This suggests that the observed heat-related risk in typically heat-protected occupations, such as law and administration, may partly reflect the underlying health profile of workers in these fields.

Figure 6: Occupational differences between the 10% of workers predicted most and 50% predicted least at risk



The figure illustrates CLAN results for 36 occupations. The bars represent the average percentage difference in the share of workers belonging to occupation groups (classified by the 2-digit codes of the KldB system) between workers in the top 10% percentile and the bottom 50% percentile of the predicted heat-absence risk. Black bars represent estimates without controlling for the age, sex and general healthcare demand of the workers, while white bars reflect estimates with these controls. The column to the left of the plot displays the difference between these estimates. The bars are plotted with 95% confidence intervals. The sample size is 2,449,830,439 in regression without and 2,415,277,838 in regressions with controls for healthcare demand.

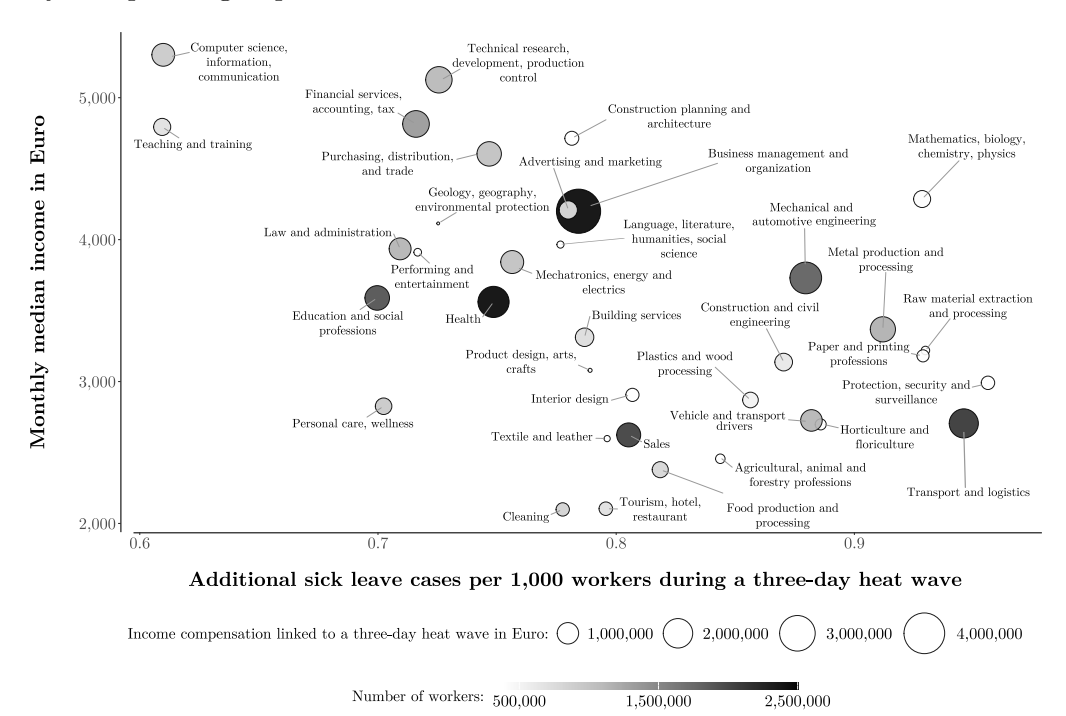
In Figure 7, we provide a back-of-the-envelope estimate of the income compensation costs paid for sick leave associated with an average three-day heat-wave for each occupation group. We quantify the costs using the formula $L_k = \sum_{j=1}^6 (\sum_{d=1}^3 \beta_{jd} s_{jk}) (N_k^f + N_k^p) \cdot I_k \cdot D$, where s_{jk} is the share of workers in occupation group k belonging to risk group j.²⁴ β_{jd} denotes the estimated effect of a heat exposure day d on sick leave for risk group j (as shown in Figure 5), N_k^f is the number of full-time and N_k^p the number of part-time workers

²⁴For every occupation group, Appendix Figure B.2 displays how the share of workers in each risk group deviates from the average share in percent. Positive values indicate that a risk group is more common in a given occupation than in the overall workforce, while negative values indicate that the group is less common.

in occupation group k, I_k is the median income in that group, and D is the average duration in days of a sick leave episode (equal to 12 days). The bubble size in Figure 7 represents the total income compensation costs per occupation group due to a three-day heatwave. The y-axis shows the median income, while the x-axis indicates the estimated increase in sick leave cases per 1,000 workers. The color shading corresponds to the number of workers in each occupation group.

Figure 7 provides two key insights. First, and most importantly, it shows that a three-day heat wave leads to additional sick leave cases across *all* occupation groups, even among those least affected. This highlights that heat affects the

Figure 7: Total sick leave income compensation payments linked to heat waves by occupation group



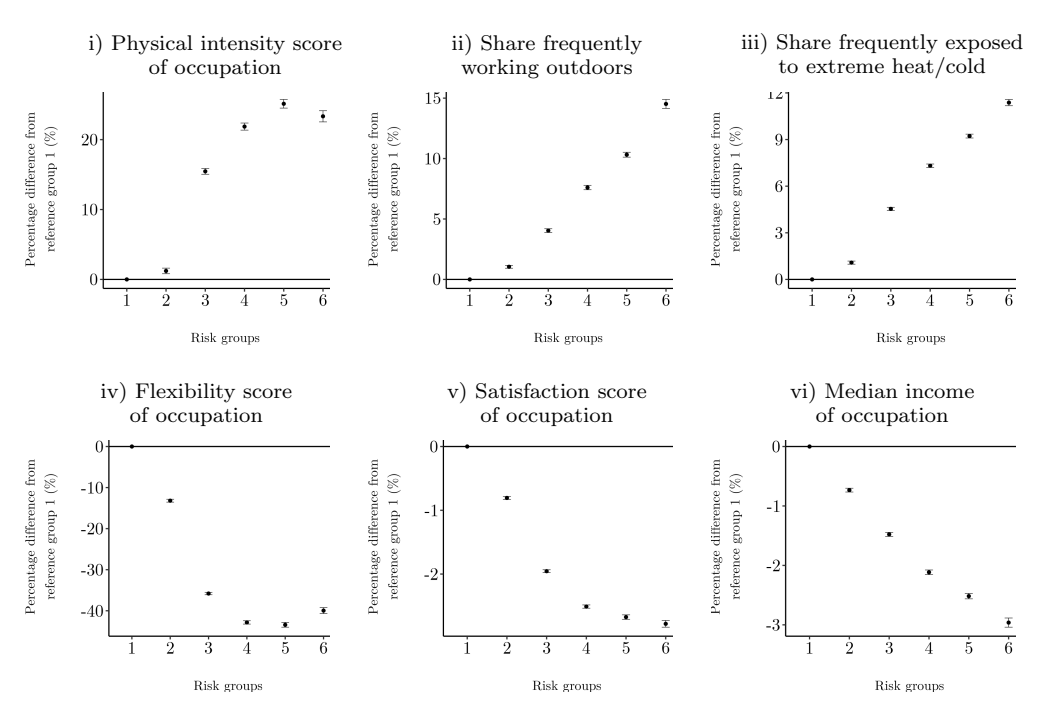
The figure shows the total sick leave income compensation payments that accumulate in the 36 occupation groups in response to an average three-day heat wave. We calculate the total costs as the product of the occupation-specific effects of a heat wave on sick leave cases, the total number of workers in each occupation group, the median income they receive, and the average duration of a sick leave case. We approximate the occupation-specific effects of a heat wave on sick leave cases based on the risk-group-specific coefficients illustrated in Figure 5 and the occupation-specific distribution of workers across these risk groups. The calculated effects represent the number of additional sick leave cases per 1,000 workers during a three-day heat wave and are illustrated on the x-axis. The y-axis represents the median income in Euro, the color of the bubbles indicates the size of the workforce, and the size of the bubbles the calculated sick leave-related income compensation costs.

entire labor force and that focusing ex-ante only on those assumed to be high-risk leads to underestimation. Second, the cost of income compensation linked to sick leave varies due to different underlying factors. For example, compensation costs in computer science, information, and communication $(1,146,020\ \mbox{\ em})$ are close to the costs for vehicle and transport drivers $(1,016,766\ \mbox{\ em})$. However, the former stems from higher median wages $(5,302\ \mbox{\ em})$ vs. $(2,726\ \mbox{\ em})$, while the latter is driven by a greater sensitivity of sick leave to heat exposure $(0.610\ \text{vs.}\ 0.882\ \text{cases}\ \text{per}\ 1,000\ \text{workers})$ and a larger workforce $(952,293\ \text{vs.}\ 1,153,009\ \text{workers})$. Overall, the highest costs are observed in business management and organization, with total compensation payments amounting to $(4,760,292\ \mbox{\ em})$. Aggregating across all occupation groups, we estimate total sick leave-related income compensations costs of $(32,230,912\ \mbox{\ em})$ for a single three-day heatwave across Germany.

The back-of-the-envelope calculation of the aggregate costs is a conservative lower bound of the full labor market impact of heatwaves. In particular, it does not account for potential disruptions to downstream industries or declines in productivity among workers who remain on the job. One occupation group that highlights the relevance of such amplifying effects is medical health professions ("health" in Figure 7). Sick leave in this group indicates a strain on the system's supply capacity. We estimate that a three-day heatwave results in approximately 0.749 additional sick leave cases per 1,000 workers in the healthcare sector. With 2,745,919 workers in this occupation group and an average sick leave duration of 12 days, a heat wave covering Germany would lead to 24,680 additional absence days by medical professionals. This reduction in staffing can lead to treatment and service shortages, potentially amplifying the health impacts of extreme heat through supply-side constraints. In line with this concern, Aguilar-Gomez et al. (2025) find that in Mexico, more than half of excess deaths during extreme heat may be linked to spillover effects from hospital congestion. A growing body of evidence more generally suggests that heat can impair cognitive functioning and decision-making (Heyes and Saberian 2019, Graff Zivin et al. 2018), indicating that the true cost of heat exposure to the labor market may be significantly higher.

Finally, Figure 8 identifies the common occupational characteristics that correlate with higher effects of heat on sick leave across professions. To this end, we examine the prevalence of six workplace characteristics (i.e. exposure to extreme temperatures, outdoor work, physical demands, job flexibility, worker satisfaction, and median income) among workers in our six risk groups shown in Figure 5, with the 50% of workers at lowest risk serving as the reference group. We find that the heat-absence risk increases with exposure to extreme temperatures and outdoor conditions, as well as the amount of physical work. Simultaneously, it decrease with the flexibility to adjust the working conditions, the satisfaction with work, and the level of income. While the relationship is monotonic in most

Figure 8: Differences in occupational characteristics between the risk groups



The figure illustrates CLAN results for six occupational characteristics. For each characteristic, the estimated coefficients represent the average percentage-point difference between workers in the six risk groups shown in Figure 5. These groups correspond to workers whose predicted heat-absence risk falls within percentile intervals beginning at the 0th (group 1), 50th (group 2), 75th (group 3), 90th (group 4), 95th (group 5), and 99th (group 6) percentiles. The six groups correspond to workers whose predicted heat-absence risk falls within percentile intervals beginning at the 0th (group 1), 50th (group 2), 75th (group 3), 90th (group 4), 95th (group 5), and 99th (group 6) percentiles. Risk groups are plotted on the x-axes. Group one with the lowest predicted risk represents the reference group. Coefficients, are plotted with 95% confidence intervals. The sample size is 4,049,603,787.

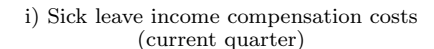
panels, it levels off in some cases. For example, the risk groups four to six share similar levels of workplace flexibility. Due to a high level of correlation among the six observed occupational characteristics and in the absence of exogenous variation, it is impossible to disentangle their individual causal impact on the heat-sick leave relationship. However, the findings provide insights for the identification of occupation groups that are more likely to call in sick on hot days, which can be informative for the design of heat protection measures. In particular, they suggest that heat disproportionately hits the already disadvantaged part of the working population.

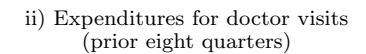
4.3 Long-term heat effects on health care expenditures

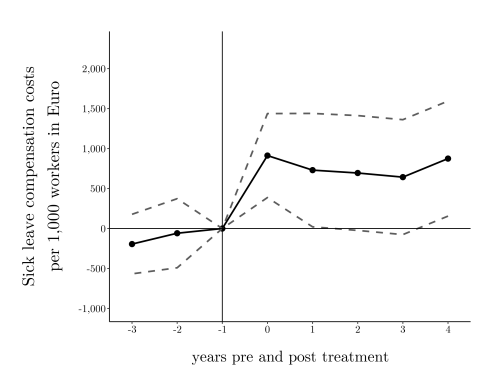
The final set of results exploits the longitudinal nature of our data and focuses on the long-term impacts of experiencing a heat wave on sick leave-related income compensation and expenditures for doctor visits. Figure 9 shows the event study estimates for the effects of an additional day of exposure to a heat wave lasting at least three days on the expenditures for (i) sick leave and (ii) doctor visits, in the years before and after the heat wave occurred. Given that certificates of work incapacity need to be issued by doctors, we expect any increase in sick leave costs to also result in higher costs for doctor visits.

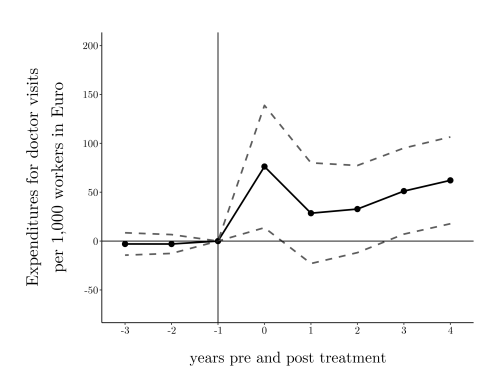
Our findings suggest a sustained increase in both outcomes following heat wave exposure. We observe an immediate uptick after the heat wave in both cases. While sick leave costs remain elevated at a consistent level, the initial increase in expenditures for doctor visits subsides after the first year, before rising again toward the later part of the observation period. This pattern could be explained by heat waves triggering the onset of severe chronic conditions, which progressively worsen over time and ultimately lead to increased long-term health care demand. However, another possible explanation is that we observe doctor expenditures in our data only as a rolling aggregate measured over the prior eight quarters. Thus, coefficients in the first years post-exposure still partially re-

Figure 9: Event-study estimates of long-term effects of heat waves on healthcare expenditures









This figure shows event study estimates of the effects of heat wave days on outcomes in the years prior and post to exposure, following Equation 3. The dependent variable refers to either the expenditures (in Euro) for (i) sick leave-related income compensation in the current quarter or (ii) the average number of outpatient treatments by a doctor over the previous eight quarters, both measured per 1,000 workers and quarter. The regressions include zip area—year and state—year—quarter fixed effects. We include controls for sex and precipitation. The regressions are weighted by the number of workers per zip-sexrisk group cell. Standard errors are clustered at the county level. Confidence intervals refer to the 5% level of significance.

flect pre-exposure measurements, potentially dampening immediate effects (see Section 3.3).

The pooled estimates of the post-treatment effects, presented in Panel A of Table A.14 in the Appendix, suggest that a heat wave day increases sick leave costs by about 0.22%, and the expenditures for doctor visits by about 0.04% in the following quarters. For a three-day heat wave, the additional costs per 1,000 workers amount to roughly 2,715 $\mbox{\ensuremath$

²⁵We obtain these values by multiplying the coefficient estimates in Table A.14 by a factor of three.

in a disproportionate increase in total sick leave days compared to the number of doctor consultations.

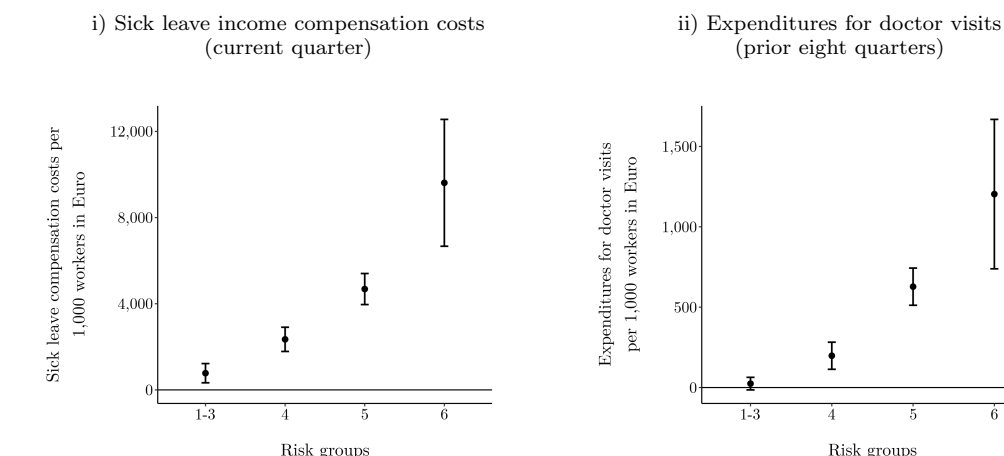
To contextualize the magnitude of these effects, we compare them to the long-term costs of a disease that typically leads to persistent health impairments requiring ongoing treatment in Appendix Section D. While statistics on such long-term costs are rarely available, we do have data on the costs occurring for ischemic stroke survivors in post-incident years. We find that exposing approximately 6,868 workers to a severe heatwave results in long-term costs for doctor visits comparable to those of all outpatient costs incurred by a single additional stroke survivor. Moreover, exposing approximately 464 workers to a severe heatwave results in long-term sick leave costs comparable to those incurred by a single additional stroke survivor.

Figure 10 presents pooled post-treatment effects by risk groups with different levels of predicted heat-absence risk (see Panel B of Table A.14 for point estimates). For both outcomes, we observe that long-term effects increase in magnitude as the predicted heat-absence risk rises. For doctor visits, statistically significant effects are found only for risk groups four, five, and six, i.e., the top 10% of workers with the highest predicted risk. In contrast, all worker groups exhibit a significant increase in expenditures for income compensation due to sick leave. Across the risk groups, the coefficients display a sharp gradient. For sick leave cases, for instance, the estimated coefficient for risk group one (the top 1%) is approximately 12 times greater than for the bottom 90%.

We provide suggestive evidence that the sustained cost increases arise through at least two channels on the extensive margin (see additional analyses for selected health conditions in Appendix Section E for more details). First, we find that heat waves can trigger the onset of new diseases, which constitute significant health shocks that typically impair workers' health and ability to work persis-

²⁶Figures B.3 and B.4 in the Appendix also provide event study estimates for sick leave days by ICD-10 chapter and gender. Long-term effects are particularly pronounced for diseases of the blood and immune system (D50–D89), the nervous system (G00–G99), and the circulatory system (I00–I99), among male workers.

Figure 10: Pooled long-term effect of heat wave exposure by risk groups



This figure illustrates estimates of the pooled long-term effect of an average heat wave day by the heatabsence risk group. The dependent variable refers to either the expenditures (in Euro) for (i) sick leave income compensation in the current quarter or (ii) the average number of outpatient treatments by a doctor over the previous eight quarters, both measured per 1,000 workers and quarter. Risk groups 1 to 3 include workers with a predicted heat-absence risk in the [0,90) percentile interval; risk group 4 corresponds to the [90,95) interval; risk group 5 to the [95,99) interval; and risk group 6 to the [99, 100] percentile interval. The regressions include zip area—year and state—year—quarter fixed effects. We include controls for sex and precipitation. The regressions are weighted by the number of workers per zip-sex-risk group cell. Confidence intervals refer to the 5% level of significance.

Ī

tently. In particular, we find that a three-day heat wave leads to a 1% increase in new diagnoses of cerebrovascular diseases (I60–I69), such as stroke. Second, heat waves have the potential to temporally exacerbate symptoms, thereby prompting individuals to seek medical attention and consequently leading to the detection of diseases that likely existed before but went undiagnosed. Supporting this potential channel, we find that a three-day heat wave leads to a 0.35% increase in new diagnoses of affective disorders (F30-F39), such as recurrent depressive episodes which typically develop more gradually over time. Once formally diagnosed, these previously untreated conditions may lead to subsequent treatments and work absences in the long-term. The potential role of heat episodes in revealing latent disease burdens is important for putting the magnitude of the long-term effects into perspective.

Overall, we suggest interpreting the findings in this section as indicative of persistent increases in healthcare demand following prolonged periods of extreme heat. While we use stringent fixed effects specifications to isolate the estimates from confounding temporal and spatial dynamics, we only observe the outcome variable on doctor visits in biennial aggregates, and we lack precision for some effect estimates. At the same time, we note that the size of the estimated effects is economically significant. This makes substantiating our tentative findings all the more important.

To this end, we conduct additional robustness checks. First, we perform a placebo test by re-estimating the event studies shown in Figure 9, while randomizing heatwave exposure across our units of observations. Appendix Figure B.5 illustrates that the sustained increases we observe in Figure 9 are no longer present. Thus, the test does not indicate apparent model misspecifications. Second, to account for potential bias linked to treatment effect heterogeneity in settings of staggered treatments (Callaway et al. 2024, Athey and Imbens 2022, Goodman-Bacon 2021, de Chaisemartin and d'Haultfoeuille 2020), we reestimate the effects using the robust estimator proposed by De Chaisemartin and d'Haultfoeuille 2024. To apply this estimator, we aggregate the data to the year-zip level and include only zip and state—year fixed effects in the regression, further limiting statistical power. We then estimate event-study effects that are normalized by the average cumulative incremental treatment dose received, and restrict the estimation to switchers for which all effects can be estimated, to avoid compositional changes. Compared to the previous results, Appendix Figure B.6 shows less clear effects and noisier pre-treatment trends, yet both outcomes still seem to rise in the post-treatment period. For both outcomes, the average cumulative total post-treatment effects are statistically significant at the 0.1% level.²⁷

5 Conclusion

This paper studies the impact of prolonged exposure to heat on sick leave among the labor force in both the short and long run. To this end, we link rich admin-

²⁷In Appendix F, we also present supplementary analyses using two additional measures of healthcare demand that proxy worker co-morbidity through pharmaceutical and hospital treatment expenditures. However, these variables come with limited informative value and the analyses do not yield meaningful additional insights.

istrative public health insurance data among German workers over more than a decade to the quasi-experimental occurrence of heat waves. Germany is an interesting case study. First, climate change has warmed up Europe more than twice as fast over the past 30 years compared to the global average (WMO 2022). Second, our study leverages an institutional setting that grants population-wide access to health care and universal statutory sick leave to shield workers from income losses due to workplace absences because of illness. In particular, we exploit individual-level sick leave data on about 9.7 million workers, with detailed information on their occupation, health status, and individual characteristics. This allows us to map how subtle health effects at the level of the individual employee aggregate to sizable economic costs and how these costs are distributed among workers.

We present strong evidence showing that sick leave increases in response to heat. A three-day heat wave covering Germany results in income compensation costs from heat-induced sick leave of about 32 million € across occupations. However, this number reflects only a fraction of the total costs of heat-induced decrease in labor supply as it neglects disruptions for downstream industries and a lower productivity in employees who are at work, for instance. We demonstrate that certain workers are particularly susceptible to heat exposure, especially those with lower income, more physically demanding tasks, and less flexibility to schedule and adjust working hours. However, even those with the lowest predicted risk of heat-related absenteeism show an increase in sick leave when heat persists for more than a day. This finding underscores that heat impacts workers across all professions, and that concentrating solely on specific occupation groups can lead to a significant underestimation of the broader heat impact. Lastly, we provide suggestive evidence for sustained increases in expenditures for sick leave and doctor visits in the years following heat wave exposure.

Our results can inform the design of climate change adaptation measures. To mitigate damages from heat today and in the future, labor markets worldwide will need to implement strategies to protect workers while ensuring production continuity. In general, this may include the provision of training and education on the risks of heat stress. More specifically, our results suggest that targeted measures may be those that reduce heat exposure (e.g., access to cooler indoor or outdoor environments and protective equipment), allow for flexible work scheduling, and explicitly address the needs of workers with at-risk morbidity profiles and those providing critical healthcare services. Our results also feed into a more general debate about the distributional implications of climate change within countries. They show that increasing heat could lead to a widening of economic and social disparities, as those who are already disadvantaged are more likely to experience negative consequences.

Our paper does not address some important aspects. First, while we provide tentative evidence of increased healthcare demand in the long run following the exposure to heat waves, this analysis is based on a smaller subset of individuals who were continuously insured and did not relocate. Moreover, we analyze longterm heat exposure effects on doctor visits measured over an extended period of eight quarters, reducing statistical power and limiting the precision of this analysis. We also note that taking sick leave, while reducing labor supply in the short term, can support long-term labor supply if it serves a protective role by preventing more severe illness. Second, while extremely high temperatures increase sick leave in the aggregate labor market, we are unable to speak to the net effect of climate change. If extremely cold temperatures also reduce the workers' ability to work and become less frequent due to climate change, our estimates for the overall impact on sick leave may be an upper bound. Third, while we identify notable heterogeneity in the effects of heat exposure on sick leave and healthcare demand, which helps guide the targeting of protection measures to those most at risk, we are unable to disentangle the specific causal pathways contributing to heat-related health risks. The lack of data on individuals' specific workplaces prevents us from accounting for workplace-specific determinants of heat susceptibility, which may vary significantly even within the same occupations. Additionally, heat may influence workers' decisions to take sick leave at a given level of illness, either because extreme conditions make supervisors more understanding or because employees may be concerned about being perceived as taking advantage of the weather.

References

- Acemoglu, D. (2002). Technical change, inequality, and the labor market. *Journal of economic literature* 40(1), pp. 7–72.
- (2024). Harms of AI. In: The Oxford Handbook of AI Governance. Oxford University Press. ISBN: 9780197579329. DOI: 10.1093/oxfordhb/9780197579329.013.65. eprint: https://academic.oup.com/book/0/chapter/411053764/chapter-ag-pdf/57890064/book/_41989_section_411053764.ag.pdf. URL: https://doi.org/10.1093/oxfordhb/9780197579329.013.65.
- Acemoglu, D. and P. Restrepo (2018). The Race between Man and Machine: Implications of Technology for Growth, Factor Shares, and Employment. *American Economic Review* 108(6), pp. 1488–1542. DOI: 10.1257/aer.20160696.
- Aguilar-Gomez, S., J. S. G. Zivin, and M. J. Neidell (2025). Killer congestion: Temperature, healthcare utilization and patient outcomes. Tech. rep. National Bureau of Economic Research.
- Almond, D. and J. Currie (2011). Killing Me Softly: The Fetal Origins Hypothesis. *Journal of Economic Perspectives* 25(3), pp. 153–172.
- Anderson, G. B. and M. L. Bell (2011). Heat waves in the United States: mortality risk during heat waves and effect modification by heat wave characteristics in 43 US communities. *Environmental Health Perspectives* 119(2), pp. 210–218.
- Athey, S. and G. W. Imbens (2022). Design-based Analysis in Difference-in-differences Settings with Staggered Adoption. *Journal of Econometrics* 226(1), pp. 62–79.
- Banerjee, R. and R. Maharaj (2020). Heat, infant mortality, and adaptation: Evidence from India. *Journal of Development Economics* 143, p. 102378.
- Barreca, A., K. Clay, O. Deschenes, M. Greenstone, and J. S. Shapiro (2016). Adapting to climate change: The remarkable decline in the US temperature-mortality relationship over the twentieth century. *Journal of Political Economy* 124(1), pp. 105–159.
- BAuA, F. (2022). Economic Costs due to Incapacity for Work 2020. URL: https://www.baua.

 de/DE/Themen/Arbeitswelt-und-Arbeitsschutz-im-Wandel/Arbeitsweltberichterstattung/
 Kosten-der-AU/Kosten-der-Arbeitsunfaehigkeit.html.
- Behrer, A. P. and J. Park (2017). Will we adapt? temperature, labor and adaptation to climate change. *Harvard Project on Climate Agreements Working Paper*, pp. 16–81.

- Bhat, B., J. De Quidt, J. Haushofer, V. H. Patel, G. Rao, F. Schilbach, and P.-L. P. Vautrey (2022). The long-run effects of psychotherapy on depression, beliefs, and economic outcomes. Tech. rep. National Bureau of Economic Research.
- BMG, F. (2022). Gesetzliche Krankenversicherung Mitglieder, mitversicherte Angehörige und Krankenstand Jahresdurchschnitt 2021, (Ergebnisse der GKV-Statistik KM1/13). URL: https://www.bundesgesundheitsministerium.de/fileadmin/Dateien/3_Downloads/Statistiken/GKV/Mitglieder_Versicherte/KM1_JD_2021_K_bf.pdf.
- Brasseur, G. P., D. Jacob, and S. Schuck-Zöller (2017). Klimawandel in Deutschland: Entwicklung, Folgen, Risiken und Perspektiven. Springer Nature.
- Breza, E., M. Kanz, and L. F. Klapper (2020). Learning to navigate a new financial technology: Evidence from payroll accounts. Tech. rep. National Bureau of Economic Research.
- Brixy, U. and A. Haas (2025). Die Wege zwischen Arbeits- und Wohnort sind seit der Covid-19-Pandemie deutlich länger geworden [website]. IAB-Forum 13. Juni 2025, [distributor]. https://iab-forum.de/die-wege-zwischen-arbeits-und-wohnort-sind-seit-der-covid-19-pandemie-deutlich-laenger-geworden/. (last accessed July, 2025).
- Burke, M., F. González, P. Baylis, S. Heft-Neal, C. Baysan, S. Basu, and S. Hsiang (2018). Higher temperatures increase suicide rates in the United States and Mexico. *Nature Climate Change* 8(8), pp. 723–729.
- Callaway, B., A. Goodman-Bacon, and P. H. Sant'Anna (2024). Difference-in-differences with a continuous treatment. Tech. rep. National Bureau of Economic Research.
- Carleton, T., A. Jina, M. Delgado, M. Greenstone, T. Houser, S. Hsiang, A. Hultgren, R. E. Kopp, K. E. McCusker, I. Nath, et al. (2022). Valuing the global mortality consequences of climate change accounting for adaptation costs and benefits. *The Quarterly Journal of Economics* 137(4), pp. 2037–2105.
- Chernozhukov, V., M. Demirer, E. Duflo, and I. Fernandez-Val (2018). Generic machine learning inference on heterogenous treatment effects in randomized experiments. Tech. rep. National Bureau of Economic Research.
- Colmer, J. and J. Voorheis (2025). The Intergenerational Effects of Early-Life Pollution Exposure. *Journal of Political Economy: Microeconomics*.
- De Chaisemartin, C. and X. d'Haultfoeuille (2020). Two-way Fixed Effects Estimators with Heterogeneous Treatment Effects. *American Economic Review* 110(9), pp. 2964–96.
- De Chaisemartin, C. and X. d'Haultfoeuille (2024). Difference-in-differences estimators of intertemporal treatment effects. *Review of Economics and Statistics*, pp. 1–45.

- Deryugina, T., G. Heutel, N. H. Miller, D. Molitor, and J. Reif (2019). The mortality and medical costs of air pollution: Evidence from changes in wind direction. *American Economic Review* 109(12), pp. 4178–4219.
- Deryugina, T. and S. M. Hsiang (2014). Does the environment still matter? Daily temperature and income in the United States. Tech. rep. National Bureau of Economic Research.
- Deschenes, O. (2011). Climate policy and labor markets. In: The design and implementation of US climate policy. University of Chicago Press, pp. 37–49.
- Deschênes, O. and M. Greenstone (2007). The economic impacts of climate change: evidence from agricultural output and random fluctuations in weather. *American Economic Review* 97(1), pp. 354–385.
- (2011). Climate change, mortality, and adaptation: Evidence from annual fluctuations in weather in the US. American Economic Journal: Applied Economics 3(4), pp. 152–185.
- Destatis (2021). Ein Krankenhausfall kostete 2019 durchschnittlich 5088 Euro, Pressemitteilung Nr. 194 vom 16. April 2021.
- Dillender, M. (2021). Climate Change and Occupational Health Are There Limits to Our Ability to Adapt? *Journal of Human Resources* 56(1), pp. 184–224.
- DIMDI (n.d.). Internationale statistische Klassifikation der Krankheiten und verwandter Gesundheitsprobleme [website]. German Institute for Medical Documentation and Information (DIMDI) [distributor]. https://www.dimdi.de/static/de/klassifikationen/icd/icd-10-gm/kode-suche/htmlgm2022/. (last accessed July, 2022).
- D'Ippoliti, D., P. Michelozzi, C. Marino, F. de'Donato, B. Menne, K. Katsouyanni, U. Kirchmayer, A. Analitis, M. Medina-Ramón, A. Paldy, et al. (2010). The impact of heat waves on mortality in 9 European cities: results from the EuroHEAT project. *Environmental Health* 9(1), pp. 1–9.
- Drescher, K. and B. Janzen (2025). When weather wounds workers: The impact of temperature on workplace accidents. *Journal of Public Economics* 241, p. 105258.
- Einav, L., A. Finkelstein, S. Mullainathan, and Z. Obermeyer (2018). Predictive Modeling of US Health Care Spending in Late Life. *Science* 360(6396). Publisher: American Association for the Advancement of Science, pp. 1462–1465.
- Federal Employment Agency (2021). Sozialversicherungspflichtige Bruttoarbeitsentgelte Deutschland, West/Ost, Länder und Kreise (Jahreszahlen), Stichtag: 31.12.2020. URL: https://statistik.arbeitsagentur.de/SiteGlobals/Forms/Suche/Einzelheftsuche_Formular.html?nn=1523076&topic_f=beschaeftigung-entgelt-entgelt.

- Flouris, A., H. Graczyk, B. Nafradi, and N. Scott (2024). Heat at Work: Implications for Safety and Health. A Global Review of the Science, Policy and Practice.
- Gensicke, M. and N. Tschersich (2018). BIBB/BAuA-Erwerbstätigenbefragung 2018. *Methodenbericht. München*.
- Goodman-Bacon, A. (2021). Difference-in-differences with variation in treatment timing. *Journal of econometrics* 225(2), pp. 254–277.
- Graff Zivin, J., S. M. Hsiang, and M. Neidell (2018). Temperature and human capital in the short and long run. *Journal of the Association of Environmental and Resource Economists* 5(1), pp. 77–105.
- Graff Zivin, J. and M. Neidell (2014). Temperature and the allocation of time: Implications for climate change. *Journal of Labor Economics* 32(1), pp. 1–26.
- Grimbuhler, S. and J.-F. Viel (2021). Heat stress and cardiac strain in French vineyard workers.

 Annals of Work Exposures and Health 65(4), pp. 390–396.
- Guryan, J., J. Ludwig, M. P. Bhatt, P. J. Cook, J. M. Davis, K. Dodge, G. Farkas, R. G. Fryer Jr, S. Mayer, H. Pollack, et al. (2023). Not too late: Improving academic outcomes among adolescents. *American Economic Review* 113(3), pp. 738–765.
- Heutel, G., N. H. Miller, and D. Molitor (2021). Adaptation and the mortality effects of temperature across US climate regions. *The Review of Economics and Statistics* 103(4), pp. 740–753.
- Heyes, A. and S. Saberian (2019). Temperature and decisions: evidence from 207,000 court cases. *American Economic Journal: Applied Economics* 11(2), pp. 238–265.
- Holub, F., L. Hospido, and U. J. Wagner (2020). Urban air pollution and sick leaves: Evidence from social security data.
- Ioannou, L. G., L. Tsoutsoubi, G. Samoutis, L. K. Bogataj, G. P. Kenny, L. Nybo, T. Kjellstrom, and A. D. Flouris (2017). Time-motion analysis as a novel approach for evaluating the impact of environmental heat exposure on labor loss in agriculture workers. *Temperature* 4(3), pp. 330–340.
- Ireland, A., D. Johnston, and R. Knott (2023). Heat and worker health. *Journal of health economics* 91, p. 102800.
- Isen, A., M. Rossin-Slater, and R. Walker (2017a). Relationship between season of birth, temperature exposure, and later life wellbeing. *Proceedings of the National Academy of Sciences* 114(51), pp. 13447–13452.

- Isen, A., M. Rossin-Slater, and W. R. Walker (2017b). Every Breath You Take Every Dollar You'll Make: The Long-Term Consequences of the Clean Air Act of 1970. Journal of Political Economy 125(3), pp. 848–902.
- Jaunzeme, J., S. Eberhard, and S. Geyer (2013). Wie repräsentativ sind GKV-Daten? Bundes-gesundheitsblatt Gesundheitsforschung -Gesundheitsschutz 56(3), pp. 447–454.
- Karlsson, M. and N. R. Ziebarth (2018). Population health effects and health-related costs of extreme temperatures: Comprehensive evidence from Germany. *Journal of Environmental Economics and Management* 91, pp. 93–117.
- KBV (2019). Honorarbericht für das vierte Quartal 2019. Kassenärztliche Bundesvereinigung: Berlin.
- Klauber, H., F. Holub, N. Koch, N. Pestel, N. Ritter, and A. Rohlf (2024). Killing prescriptions softly: Low emission zones and child health from birth to school. *American Economic Journal: Economic Policy* 16(2), pp. 220–248.
- Kolominsky-Rabas, P. L., P. U. Heuschmann, D. Marschall, M. Emmert, N. Baltzer, B. Neundorfer, O. Schoffski, and K. J. Krobot (2006). Lifetime cost of ischemic stroke in Germany: results and national projections from a population-based stroke registry: the Erlangen Stroke Project. Stroke 37(5), pp. 1179–1183.
- Krause, M. and S. Kripfganz (2025). Regional dependencies and local spillovers: Insights from commuter flows. *Journal of Regional Science*.
- LoPalo, M. (2023). Temperature, worker productivity, and adaptation: evidence from survey data production. *American Economic Journal: Applied Economics* 15(1), pp. 192–229.
- Marschall, J., S. Hildebrandt, H. Sydow, H.-D. Nolting, E Burgart, and T Woköck (2017). Gesundheitsreport 2017. medhochzwei-Verlag.
- Miller, S., K. Chua, J. Coggins, and H. Mohtadi (2021). Heat waves, climate change, and economic output. *Journal of the European Economic Association* 19(5), pp. 2658–2694.
- Mullins, J. T. and C. White (2019). Temperature and mental health: Evidence from the spectrum of mental health outcomes. *Journal of health economics* 68, p. 102240.
- NWS, N. (2024a). The Heat Index Equation. URL: http://www.wpc.ncep.noaa.gov/html/heatindex_equation.shtml.
- (2024b). Understanding Wind Chill. URL: https://www.weather.gov/safety/cold-wind-chill-chart.

- Obradovich, N., R. Migliorini, M. P. Paulus, and I. Rahwan (2018). Empirical evidence of mental health risks posed by climate change. *Proceedings of the National Academy of Sciences* 115(43), pp. 10953–10958.
- Park, J., N. Pankratz, and A. Behrer (2021). Temperature, workplace safety, and labor market inequality.
- Park, R. J., J. Goodman, M. Hurwitz, and J. Smith (2020). Heat and learning. *American Economic Journal: Economic Policy* 12(2), pp. 306–39.
- Sanders, N. J. (2012). What Doesn't Kill You Makes You Weaker: Prenatal Pollution Exposure and Educational Outcomes. *Journal of Human Resources* 47(3), pp. 826–850.
- Simeonova, E., J. Currie, P. Nilsson, and R. Walker (2019). Congestion Pricing, Air Pollution and Children's Health. *Journal of Human Resources*, 0218–9363R2.
- Skajaa, N., K. Adelborg, E. Horváth-Puhó, K. J. Rothman, V. W. Henderson, L. C. Thygesen, and H. T. Sørensen (2023). Labour market participation and retirement after stroke in Denmark: registry based cohort study. *bmj* 380.
- Swart, E., P. Ihle, H. Gothe, and D. Matusiewicz (2014). Routinedaten im Gesundheitswesen: Handbuch Sekundärdatenanalyse: Grundlagen, Methoden und Perspektiven. Hogrefe AG.
- Tannis, C. (2020). Heat illness and renal injury in mail and package delivery workers. *American journal of industrial medicine*.
- Wilson, A. J., R. D. Bressler, C. Ivanovich, C. Tuholske, C. Raymond, R. M. Horton, A. Sobel, P. Kinney, T. Cavazos, and J. G. Shrader (2024). Heat disproportionately kills young people: Evidence from wet-bulb temperature in Mexico. Science Advances 10(49), eadq3367. DOI: 10.1126/sciadv.adq3367. eprint: https://www.science.org/doi/pdf/10.1126/sciadv.adq3367. URL: https://www.science.org/doi/abs/10.1126/sciadv.adq3367.
- Wissenschaftliches Institut der AOK (2020). Der GKV-Arzneimittelmarkt: Klassifikation, Methodik und Ergebnisse 2020.
- WMO (2022). State of the Climate in Europe 2021. WMO-No. 1304.
- WorldPop Hub (2018). Global High Resolution Population Denominators Project. URL: www.worldpop.org.
- Zhang, P., O. Deschenes, K. Meng, and J. Zhang (2018). Temperature effects on productivity and factor reallocation: Evidence from a half million Chinese manufacturing plants. *Journal of Environmental Economics and Management* 88, pp. 1–17.

APPENDIX

A Tables

Table A.1: Descriptive statistics on sick leave

	Me	ean value of th	e
	(1)	(2)	(3)
	sick leave	number of	duration
	cases per	sick	of sick
	1,000	workers	leave
	workers	per $1,000$	cases in
	and day	and day	days
Age and sex			
Working men			
25-35 years old	4.265	35.738	8.292
35-50 years old	3.884	47.155	11.782
50-60 years old	3.964	70.677	16.178
Working women			
25-35 years old	4.776	37.615	7.696
35-50 years old	4.306	50.732	11.220
50-60 years old	4.182	71.791	15.385
Disease groups (ICD-10)			
A00–B99: Infectious and parasitic diseases	0.401	2.620	6.395
C00–D48: Neoplasms	0.061	2.185	24.033
D50–D89: Blood, blood-forming organs, immune mechanism	0.008	0.297	21.203
E00–E90: Endocrine, nutritional and metabolic diseases	0.041	1.297	20.534
F00–F99: Mental and behavioural disorders	0.217	6.510	23.730
G00–G99: Diseases of nervous system	0.115	2.189	15.220
H00–H59: Diseases of eye and adnexa	0.052	0.471	7.866
H60–H95: Diseases of ear and mastoid process	0.056	0.583	9.358
I00–I99: Diseases of circulatory system	0.150	3.497	17.901
J00–J99: Diseases of respiratory system	1.125	8.348	7.268
K00–K93: Diseases of digestive system	0.452	3.411	6.913
L00–L99: Diseases of skin and subcutaneous tissue	0.068	0.959	12.489
M00–M99: Musculoskeletal system and connective tissue	0.867	16.085	16.064
N00-N99: Diseases of genitourinary system	0.104	1.350	11.540
O00–O99: Pregnancy, childbirth and the puerperium	0.042	0.468	10.969
Q00–Q99: Congenital body and chromosomal abnormalities	0.007	0.190	20.050
S00–T98: Injury, poisoning and other external causes	0.322	7.166	20.081
V01–Y98: External causes of morbidity and mortality	0.000	0.007	21.011

This table reports the mean daily values per 1,000 workers for: (1) new sick leave cases, (2) total sick workers, and (3) the duration of a sick leave case in days.

Table A.2: Binary variables describing workers' morbidity status in previous eight quarters

No.	ICD-10 code	Variable description
1	C00-C14	Malignant neoplasms of lip, oral cavity and pharynx
2	C15-C26	Malignant neoplasms of digestive organs
3	C30-C39	Malignant neoplasms of respiratory and intrathoracic organs
4	C40-C41	Malignant neoplasms of bone and articular cartilage
5	C43-C44	Melanoma and other malignant neoplasms of skin
6	C45-C49	Malignant neoplasms of mesothelial and soft tissue
7	C50	Malignant neoplasm of breast
8	C51-C58	Malignant neoplasms of female genital organs
9	C60-C63	Malignant neoplasms of male genital organs
10	C64-C68	Malignant neoplasms of urinary tract
11	C69-C72	Malignant neoplasms of eye, brain and other parts of CNS
12	C73-C75	Malignant neoplasms of thyroid and other endocrine glands
13	C76-C80	Malignant neoplasms of ill-defined, secondary and unspecified sites
14	C81-C96	Malignant neoplasms of lymphoid, hematopoietic and related tissue
15	C97	Malignant neoplasms of independent multiple sites
16	D00-D09	In situ neoplasms
17	E10-E14	Diabetes mellitus
18	E65-E68	Obesity and other hyperalimentation
19	F00-F09	Organic mental disorders
20	F10-F19	Mental and behavioural disorders due to psychoactive substance use
21	F20-F29	Schizophrenia, schizotypal and delusional disorders
22	F30-F39	Affective disorders
23	F40-F48	Neurotic, stress-related and somatoform disorders
24	F50-F59	Behavioural syndromes associated with physiological disturbances
		and physical factors
25	F60-F69	Disorders of adult personality and behaviour
26	F70-F79	Mental retardation
27	F80-F89	Disorders of psychological development
28	F90-F98	Behavioural and emotional disorders with onset usually occurring in
		childhood and adolescence
29	F99	Unspecified mental disorder
30	I00-I02	Acute rheumatic fever
31	I05-I09	Chronic rheumatic heart diseases
32	I10-I15	Hypertensive diseases
33	I20-I25	Ischaemic heart diseases
34	I26-I28	Pulmonary heart disease and diseases of pulmonary circulation
35	I30-I52	Other forms of heart disease
36	I60-I69	Cerebrovascular diseases

No.	Variable	Description
37	170-179	Diseases of arteries, arterioles and capillaries
38	I80-I89	Diseases of veins, lymphatic vessels and lymph nodes
39	I95-I99	Other and unspecified disorders of the circulatory system
40	J00-J06	Acute upper respiratory infections
41	J09-J18	Influenza and pneumonia
42	J20-J22	Other acute lower respiratory infections
43	J30-J39	Other diseases of upper respiratory tract
44	J40-J47	Chronic lower respiratory diseases
45	J60-J70	Lung diseases due to external agents
46	J80-J84	Other respiratory diseases principally affecting the interstitium
47	J85-J86	Suppurative and necrotic conditions of lower respiratory tract
48	J90-J94	Other diseases of pleura
49	J95-J99	Other diseases of the respiratory system
50	M00-M03	Infectious arthropathies
51	M05-M14	Inflammatory polyarthropathies
52	M15-M19	Arthrosis
53	M20-M25	Other joint disorders
54	M30-M36	Systemic connective tissue disorders
55	M40-M43	Deforming dorsopathies
56	M45-M49	Spondylopathies
67	M50-M54	Other dorsopathies
68	O80-O82	Delivery

This table presents the morbidity variables used as input features in the gradient-boosted decision tree model described in Section 3.2. All variables are available at the worker-quarter level. The binary indicators represent the presence of various diseases during the previous eight quarters, classified according to ICD-10 codes.

Table A.3: Dimensions captured by residential zip code variables

No.	Characteristic	Description	Year	Source
1	Socioeconomic status	Proportion of households in the zip code area belonging to one of seven socioeconomic	2019	Acxion
		status classes		
2	Ambulance stations	Absolute number and number per 1,000	2023	OSM
		inhabitants in zip area of ambulance stations		
		storing emergency supplies		
3	Hospitals	Absolute number and number per 1,000	2023	OSM
		inhabitants in zip area of hospitals		
4	Clinics	Absolute number and number per 1,000	2023	OSM
		inhabitants in zip area of medical centres		
		(have more staff than a doctor's office, but do		
		not admit inpatients)		
5	Doctors	Absolute number and number per 1,000	2023	OSM
		inhabitants in zip area of doctor offices		
6	Pharmacies	Absolute number and number per 1,000	2023	OSM
		inhabitants in zip area of pharmacies		
7	Playgrounds	Absolute number and number per 1,000	2023	OSM
		inhabitants in zip area of children's		
		playgrounds		
3	Public baths	Absolute number and number per 1,000	2023	OSM
		inhabitants in zip area of public baths		
9	Fitness centers	Absolute number and number per 1,000	2023	OSM
		inhabitants in zip area of fitness centers		
10	Outdoor fitness	Absolute number and number per 1,000	2023	OSM
	stations	inhabitants in zip area of outdoor facilities for		
		street workouts (e.g. calisthenics parks, trim		
		trails)		
11	Pitchs	Absolute number and number per 1,000	2023	OSM
		inhabitants in zip area in zip area pitches		
		(e.g. tennis courts, basketball courts, ball		
		parks, and riding arenas)		
12	Sports halls	Absolute number and number per 1,000	2023	OSM
		inhabitants in zip area of sports hall for		
		indoor sports indoor		
13	Tracks	Absolute number and number per 1,000	2023	OSM
		inhabitants in zip area of tracks for running,		
		cycling and other non-motorised racing		

No.	Characteristic	Description	Year	Source
14	Universities	Absolute number and number per 1,000	2023	OSM
		inhabitants in zip area of university buildings		
		(higher education)		
15	Colleges	Absolute number and number per 1,000	2023	OSM
		inhabitants in zip area of colleges buildings		
		(further education/continuing education)		
16	Social facilities	Absolute number and number per 1,000	2023	OSM
		inhabitants in zip area of social facilities (e.g.		
		drug clinics, workshops for physically		
		disabled people, homeless shelters)		
17	Commercial area	Absolute area of land used for commercial	2023	OSM
		purposes in square meters, and its share		
		relative to the total area of the zip code		
18	Constructions	Absolute area of land being built on in square	2023	OSM
		meters, and its share relative to the total area		
		of the zip code		
19	Farmland	Absolute area of farmland used for tillage in	2023	OSM
		square meters, and its share relative to the		
		total area of the zip code		
20	Forest	Absolute area of forest or woodland in square	2023	OSM
		meters, and its share relative to the total area		
		of the zip code		
21	Gardens	Absolute area of garden in square meters, and	2023	OSM
		its share relative to the total area of the zip		
		code		
22	Industrial area	Absolute area of land used for industrial	2023	OSM
		purposes in square meters, and its share		
		relative to the total area of the zip code		
23	Nature reserves	Absolute area of protected nature in square	2023	OSM
		meters, and its share relative to the total area		
		of the zip code		
24	Parks	Absolute area of parks in square meters, and	2023	OSM
		its share relative to the total area of the zip		
		code		
25	Recreation ground	Absolute area for general recreation in square	2023	OSM
	-	meters, and its share relative to the total area		
		of the zip code		
26	Residential area	Absolute area in primary use by humans in	2023	OSM
		square meters, and its share relative to the		
		total area of the zip code		

No.	Characteristic	Description	Year	Source
27	Retail area	Absolute area used predominantly for shops	2023	OSM
		in square meters, and its share relative to the		
		total area of the zip code		
28	Water	Absolute area of all inland bodies of water	2023	OSM
		(naturally occurring and man made) in		
		square meters, and its share relative to the		
		total area of the zip code		
29	Coastline	Absolute length of coastline in meters and	2023	OSM
		length per inhabitants in zip area		
30	Age	Average age in years and age distribution by	2011	Census
		age group (<10, 10–19, 20–29,, 80+) of the		
		population in years and percentage share of		
		people		
31	Share of foreigners	Percentage share of foreigners in the total	2011	Census
		population		
32	Country of birth	Percentage share of persons by birth country	2011	Census
	v	(Germany, EU-27, other Europe, other world,		
		unknown)		
33	Citizenship	Percentage share of persons by citizenship	2011	Census
	•	across regions (Germany, EU-27, other		
		Europe, other world, unknown) and for		
		selected countries (e.g. Bosnia and		
		Herzegovina, Greece, Italy)		
34	Number of citizenships	Percentage share of persons by number of	2011	Census
01	rumber of creizensmps	citizenship (one, several foreign, German and	2011	Consus
		foreign, unknown)		
35	Household size	Average number of individuals belonging to	2011	Census
00	Household Size	one household and percentage share of	2011	Consus
		households by number of persons (1 to 6+		
		persons)		
36	Household type	Percentage share of households by type	2011	Census
50	Household type	(couples without children, without children,	2011	Census
		single parents, multi-person non-family)		
37	Size of nuclear family	Percentage share of households by family size	2011	Census
01	olze of fideless family		2011	Census
38	Family type	(2 to 6+ persons) Percentage share of households by family	2011	Census
90	ranny type	types (categorized by relationship status and	2011	Census
30	Sonior citizan status	child presence)	2011	Concre
39	Senior citizen status	Percentage share of households with senior	2011	Census
		citizens (only senior citizens, with senior		
		citizens, no senior citizens)		

No.	Characteristic	Description	Year	Source
40	Flat vacancy	Proportion of flats that are vacant	2011	Census
41	Living space per	Average living space per resident in square	2011	Census
	inhabitant	meters		
42	Marital status	Percentage share of people by marital status	2011	Census
		(e.g. married, widowed, divorced,		
		registered-partnership)		
43	Sex	Percentage share of persons by sex (male,	2011	Census
		female)		
44	Religion	Percentage share of people by religion (roman	2011	Census
		catholic church, protestant church, unknown) $$		
45	Construction year	Percentage share of buildings and flats by	2011	Census
		built year (<1919 to >2009))		
46	Ownership type	Percentage share of buildings and flats by	2011	Census
		owner type (e.g. private, community, state)		
47	Type of building	Percentage share of buildings by type (e.g.	2011	Census
		residential, dormitories)		
48	Building type size	Percentage share of buildings and flats by	2011	Census
		type (e.g. detached single family house,		
		multi-family house)		
49	Type of heating	Percentage share of buildings and flats by	2011	Census
		type of heating (district, floor, block, central,		
		single/multi-room furnaces, none)		
50	Occupancy type	Percentage share of apartments by occupancy	2011	Census
		type (e.g. owned, rented, leisure, vacant)		
51	Number of rooms	Percentage share of apartments by number of	2011	Census
		rooms $(1 \text{ to } 7+)$		
52	Apartment size	Percentage share of apartments by size in	2011	Census
		square meters ($<30, 30-39, 40-49,, 180+$)		

This table reports the time-invariant characteristics of workers' residential zip codes used as input features in the gradient-boosted decision tree model described in Section 3.2. All variables are available at the zip code level for the year indicated in the table. The data come from Acxiom, OpenStreetMap (OSM), and the 2011 census from the Federal Statistical Office. The listed characteristics summarize the dimensions included in the model; each characteristic may be measured using multiple underlying variables.

Table A.4: Descriptive statistics on heat

	(1)	(2)	(2)	(4)
	(1)	(2)	(3)	(4)
	mean	sd	min	max
Heat days				
Number of heat days	5.227	4.983	0.000	28.000
Apparent heat days				
Number of apparent heat days	4.895	4.324	0.000	26.000
Tropical nights				
Number of tropical nights	2.132	3.092	0.000	23.000
Heat intensity				
Minimum heat temperature (°C)	30.348	0.770	25.749	35.168
Mean heat temperature (°C)	31.318	0.862	25.985	35.168
Maximum heat temperature (°C)	32.584	1.750	25.985	39.156
Heat duration				
Number of 1 heat day in a row	2.814	2.238	0.000	13.000
Number of 2 heat days in a row	1.274	1.392	0.000	8.000
Number of 3 heat days in a row	0.596	0.836	0.000	5.000
Number of 4 heat days in a row	0.301	0.562	0.000	3.000
Number of 5 heat days in a row	0.119	0.339	0.000	3.000
Number of 6 heat days in a row	0.059	0.235	0.000	2.000
Number of 7 heat days in a row	0.029	0.166	0.000	1.000
Number of 8 heat days in a row	0.018	0.132	0.000	1.000
Number of 9 or more heat days in a row	0.018	0.204	0.000	4.000

The table reports summary statistics on the occurrence of heat by year and zip code area for our study period (2007–2020) covering 8,174 German zip code areas. We present statistics for: (i) the total number of heat days ($\geq 30^{\circ}$ C) per year and zip code area, (ii) the total number of apparent heat days, (iii) the number of tropical nights, (iv) the minimum, mean, and maximum temperatures during heat periods (heat intensity), and (v) the number of consecutive heat days ranked from the 1st to the 9th day or more with temperatures $\geq 30^{\circ}$ C (heat duration).

Table A.5: Employment survey questions

Number	Question
(i)	Heat/cold exposure
$F600_05$	How often do they work under cold, heat, wet, damp or draught ?
(ii)	Outdoor exposure
F600	Do you work outdoors for more than half of your working hours?
(iii)	Physical work
$F600_01$	How often do you work while standing?
$F600_03$	How often do you lift or carry loads greater than $20 \mathrm{kg}$ (men)/ $10 \mathrm{kg}$ (women)?
$F600_01$	How often do you have to use your hands to perform tasks that require high skillfulness,
	rapid sequences of movements, or greater forces?
$F600 _01$	How often do you work in a stooped, squatting, kneeling position or overhead?
(iv)	Flexibility
$F700_02$	How often does it happen that you can plan and schedule your own work?
$F700_03$	How often does it happen that you have influence over the amount of work assigned to
	you?
(v)	Satisfaction
$F700_06$	How often does it happen that you can decide for yourself when to take a break?
F1451	How satisfied are you with your work overall?

This table lists the questions from the survey of the Federal Institute for Vocational Education and Training (Gensicke and Tschersich 2018), based on which we characterize the occupations groups in our analysis. We match the questions to five dimensions capturing to what extent employees (i) work under very high and very low temperatures, (ii) work outdoors, (iii) perform physically demanding tasks, (iv) are free to schedule and adjust their working hours, and (v) are satisfied with their job.

Table A.6: Lagged effects of heat days on sick leave

	Sick leave	cases per 1,000	workers
	(1)	(2)	(3)
Heat day	0.091***	0.098***	0.096***
s.e.	(0.009)	(0.009)	(0.009)
r.e.	[2.261]	[2.431]	[2.379]
Day 1 after heat day	0.097***	0.091***	0.091***
s.e.	(0.009)	(0.009)	(0.009)
r.e.	[2.420]	[2.269]	[2.262]
Day 2 after heat day		0.027***	0.029***
s.e.		(0.006)	(0.006)
r.e.		[0.671]	[0.710]
Day 3 after heat day			-0.008
s.e.			(0.006)
r.e.			[-0.194]

This table reports estimates of the effect of an average heat day on the days In stable reports estimates of the effect of an average heat day on the days following the heat day. The dependent variable refers to new sick leave cases per 1,000 workers. In all regressions, we include controls for age, sex, public holidays, and precipitation as well as year x week, zip x month, day-of-the-week x month, and day-of-the-year fixed effects. The regressions are weighted by the number of workers per zip-age-gender cell. Standard errors in round parentheses are clustered at the county level. Relative effects in percent are in square parentheses. The sample size is 57, 292, 664 . * p < .05, ** p < .01, *** p < .001.

Table A.7: Different measures of heat exposure

	Sick leave cases per 1,000 workers		
	(1)	(2)	(3)
Regular temperature	0.095***	0.146***	0.152***
s.e.	(0.015)	(0.016)	(0.016)
r.e.	[2.217]	[3.409]	[3.546]
	(4)	(5)	(6)
Apparent heat day	0.120***	0.192***	0.174***
s.e.	(0.013)	(0.012)	(0.013)
r.e.	[2.792]	[4.475]	[4.064]
	(7)	(8)	(9)
Tropical night	0.070***	0.081***	0.100***
s.e.	(0.017)	(0.016)	(0.016)
r.e.	[1.638]	[1.903]	[2.347]
		Fixed effects	
year x week	yes	yes	yes
zip	yes	no	no
day-of-the-week	yes	no	no
zip x month	no	yes	yes
day-of-the-week x month	no	yes	yes
day-of-the-year	no	no	yes

This table reports estimates of the effect of an average heat day on sick leave following Equation (1). The dependent variable refers to new sick leave cases per 1,000 workers. Panel A reports the effect of a heat day, defined using regularly measured temperatures as in Table 1. Panel B reports the effect of heat days defined using apparent temperatures, which account for humidity. Panel C reports the effect of a tropical night, defined as a night in which the minimum temperature does not fall below $20^{\circ}\mathrm{C}$. In all regressions, we include controls for age, sex, public holidays, and precipitation. The regressions are weighted by the number of workers per zip-age-gender cell. Standard errors in round parentheses are clustered at the county level. Relative effects in percent are in square parentheses. The sample size is 13, 293, 949 in Panel A, 13, 075, 890 in Panel B, and 11, 283, 177 in Panel C. * p < .05, ** p < .01, *** p < .001.

Table A.8: Different forms of heat exposure

Heat duration		Heat intensity	
	(1)		(2)
Heat day 1	0.154***	T <= 30.5°C	0.148***
s.e.	(0.016)	s.e.	(0.017)
r.e.	[3.579]	r.e.	[3.448]
Heat day 2	0.133***	$T \in (30.5^{\circ}, 31.0^{\circ}C]$	0.151***
s.e.	(0.017)	s.e.	(0.021)
r.e.	[3.098]	r.e.	[3.513]
Heat day 3	0.215***	$T \in (31.0^{\circ}C, 31.5^{\circ}C]$	0.166***
s.e.	(0.021)	s.e.	(0.020)
r.e.	[5.010]	r.e.	[3.874]
Heat day 4	0.170***	$T \in (31.5^{\circ}C, 32.0^{\circ}C]$	0.162***
s.e.	(0.024)	s.e.	(0.019)
r.e.	[3.961]	r.e.	[3.777]
Heat day 5	0.250***	$T \in (32.0^{\circ}C, 32.5^{\circ}C]$	0.129***
s.e.	(0.037)	s.e.	(0.021)
r.e.	[5.817]	r.e.	[3.010]
Heat day 6	0.170***	$T \in (32.5^{\circ}C, 33.0^{\circ}C]$	0.125***
s.e.	(0.038)	s.e.	(0.022)
r.e.	[3.952]	r.e.	[2.922]
Heat day 7	0.236***	$T \in (33.0^{\circ}C, 33.5^{\circ}C]$	0.125***
s.e.	(0.049)	s.e.	(0.024)
r.e.	[5.505]	r.e.	[2.903]
Heat day 8	0.463***	$T \in (33.5^{\circ}C, 34.0^{\circ}C]$	0.119***
s.e.	(0.065)	s.e.	(0.022)
r.e.	[10.787]	r.e.	[2.783]
Heat day 9	0.476***	T > 34.0°C	0.028
s.e.	(0.085)	s.e.	(0.022)
r.e.	[11.089]	r.e.	[0.642]

This table reports how the effects of heat vary by (1) duration of exposure (i.e. the number of consecutive heat days) and (2) intensity of exposure (i.e. the temperature of a heat day). The dependent variable is the number of new sick leave cases per 1,000 workers. The regressions include zip area—month, year—week, day-of-the-week—month, and day-of-the-year fixed effects. We include controls for age, sex, public holidays, and precipitation. The regressions are weighted by the number of workers per zip-age-gender cell. Standard errors are clustered at the county level. The sample size is 13,293,949. * p < .05, ** p < .01, *** p < .001.

Table A.9: Adding controls for vacation days

	Sick leave cases per 1,000 workers				
	Panel A: Including controls for vacation days				
	(1)	(2)	(3)		
Heat day	0.088***	0.145***	0.148***		
s.e.	(0.015)	(0.016)	(0.016)		
r.e.	[2.049]	[3.381]	[3.438]		
	Panel B: Including separate controls by vacation type				
	(4)	(5)	(6)		
Heat day	0.098***	0.153***	0.154***		
s.e.	(0.016)	(0.016)	(0.016)		
r.e.	[2.289]	[3.575]	[3.591]		
		Fixed effects			
year x week	yes	yes	yes		
zip	yes	no	no		
day-of-the-week	yes	no	no		
zip x month	no	yes	yes		
day-of-the-week x month	no	yes	yes		
day-of-the-year	no	no	yes		

This table replicates Table 1 with additional controls for vacation days. Panel A regressions include one dummy variable that equals one if the day of observation is a vacation day. Panel B regressions include five dummy variables that are equal to one if the day of observation coincides with winter, spring, pentecost, summer, fall, or winter vacation respectively. Fixed effects become more stringent from column (1) to (3). The dependent variable refers to new sick leave cases per 1,000 workers. In all regressions, we include controls for age, sex, public holidays, and precipitation. The regressions are weighted by the number of workers per zip-age-gender cell. Standard errors in round parentheses are clustered at the county level. Relative effects in percent are in square parentheses. The sample size is 13,293,949. * p<.05, ** p<.01, *** p<.001.

Table A.10: Restricting the sample to summer months $\,$

	Sick leave cases per 1,000 workers		
	(1)	(2)	(3)
Heat day	0.146***	0.124***	0.136***
s.e.	(0.012)	(0.012)	(0.013)
r.e.	[4.078]	[3.465]	[3.815]
		Fixed effects	
year x week	yes	yes	yes
zip	yes	no	no
day-of-the-week	yes	no	no
zip x month	no	yes	yes
day-of-the-week x month	no	yes	yes
day-of-the-year	no	no	yes

This table replicates Table 1 while restricting the sample to the summer months May through September. Fixed effects become more stringent from column (1) to (3). The dependent variable refers to new sick leave cases per 1,000 workers. In all regressions, we include controls for age, sex, public holidays, and precipitation. The regressions are weighted by the number of workers per zip-age-gender cell. Standard errors in round parentheses are clustered at the county level. Relative effects in percent are in square parentheses. The sample size is 13,077,280 . * p < .05, ** p < .01, *** p < .001.

Table A.11: ICD-10 disease groups

Chapter	ICD-10 code	Group name	Figure label
I	A00-B99	Infectious and parasitic diseases	Infectious diseases
II	C00-D48	Neoplasms	Neoplasms
III	D50-D89	Blood, blood-forming organs, immune mechanism	Blood & immune mechanism
IV	E00-E90	Endocrine, nutritional and metabolic diseases	Endocrine & metabolic
V	F00-F99	Mental and behavioural disorders	Mental disorders
VI	G00-G99	Diseases of nervous system	Nervous system
VII	H00-H59	Diseases of eye and adnexa	Eye diseases
VIII	H60-H95	Diseases of ear and mastoid process	Ear diseases
IX	I00-I99	Diseases of circulatory system	Circulatory system
X	J00-J99	Diseases of respiratory system	Respiratory system
XI	K00-K93	Diseases of digestive system	Digestive system
XII	L00-L99	Diseases of skin and subcutaneous tissue	Skin & subcutaneous tissue
XIII	M00-M99	Musculoskeletal system and connective tissue	Musculoskeletal system
XIV	N00-N99	Diseases of genitourinary system	Genitourinary system
XV	O00-O99	Pregnancy, childbirth and the puerperium	Pregnancy & childbirth
XVI	P00-P96	Conditions originating in the perinatal period	Perinatal conditions
XVII	Q00-Q99	Congenital body and chromosomal abnormalities	Congenital abnormalities
XIX	S00-T98	Injury, poisoning and other external causes	Injury & poisoning
XX	V01-Y98	External causes of morbidity and mortality	External causes

This table provides an overview of how the diseases listed in Figure 4 are defined in terms of ICD-10 codes.

Table A.12: CLAN results comparing high-risk and low-risk workers $\,$

	Absolute	Absolute differences	
	coef.	s.e.	
Age (in years)	1.564	(0.007)	
Female share	-0.072	(0.001)	
Number of doctor visits (last 8 quarters)	4.084	(0.006)	
	Relative dif	ferences (%)	
	coef.	s.e.	
Cancer (ICD-10: C00-D09)	47.793	(0.027)	
Diabetes (ICD-10: E10-E14)	40.922	(0.019)	
Adiposity (ICD-10: E65-E68)	33.356	(0.015)	
Affective disorders (ICD-10: F30-F39)	48.242	(0.015)	
High blood pressure (ICD-10: I10-I15)	23.470	(0.009)	
Cerebrovascular diseases (ICD-10: I60-I69)	56.464	(0.037)	
Acute respiratory diseases (ICD-10: J00-J22)	18.993	(0.007)	
Chronic respiratory diseases (ICD-10: J40-J47)	39.260	(0.010)	
Arthritis (ICD-10: M00-M25)	24.844	(0.012)	
Diseases of spine and back (ICD-10: M40-M54)	29.461	(0.010)	

The table reports CLAN regression estimates comparing workers in the top decile [90,100] of the predicted heat-absence risk distribution to those in the bottom half [0,50). All regressions except the first two include controls for age and sex. The upper panel presents absolute differences in demographic and healthcare-related variables. The lower panel reports relative differences in the prevalence of chronic conditions to facilitate comparison across diseases with differing baseline frequencies. All differences are statistically significant at the 0.1% level.

Table A.13: Differences in occupational characteristics between the risk groups

	(i) Share	(ii) Share	(iii)	(iv)	(v) Satis-	(vi)
	frequently	frequently	Physical	Flexibility	faction	Median
	exposed	working	intensity	score of	score of	income of
	to	outdoors	score of	occupa-	occupa-	occupa-
	extreme		occupa-	tion	tion	tion
	heat/cold		tion			
Risk group 2: [50, 75)	1.081***	1.046***	1.215***	-13.193***	-0.807***	-0.734***
s.e.	(0.051)	(0.062)	(0.206)	(0.177)	(0.012)	(0.016)
Risk group 3: [75, 90)	4.538***	4.040***	15.464***	-35.804***	-1.955***	-1.478***
s.e.	(0.054)	(0.079)	(0.210)	(0.147)	(0.011)	(0.017)
Risk group 4: [90, 95)	7.314***	7.603***	21.870***	-42.836***	-2.510***	-2.116***
s.e.	(0.057)	(0.093)	(0.259)	(0.207)	(0.013)	(0.020)
Risk group 5: [95, 99)	9.224***	10.319***	25.132***	-43.419***	-2.675***	-2.517***
s.e.	(0.063)	(0.102)	(0.316)	(0.292)	(0.018)	(0.024)
Risk group 6: [99, 100]	11.377***	14.521***	23.339***	-39.958***	-2.780***	-2.962***
s.e.	(0.103)	(0.189)	(0.409)	(0.371)	(0.027)	(0.039)

The table reports CLAN results. The estimated coefficients indicate the average percentage difference between workers in the six risk groups illustrated in Figure 5, i.e. groups with the 0th, 50th, 75th, 90th, 95th, and 99th percentiles as lower interval bounds. Group one with the lowest predicted risk in the quantile [0,50) represents the reference group. The sample size is 4,049,603,787. * p < .01, *** p < .001.

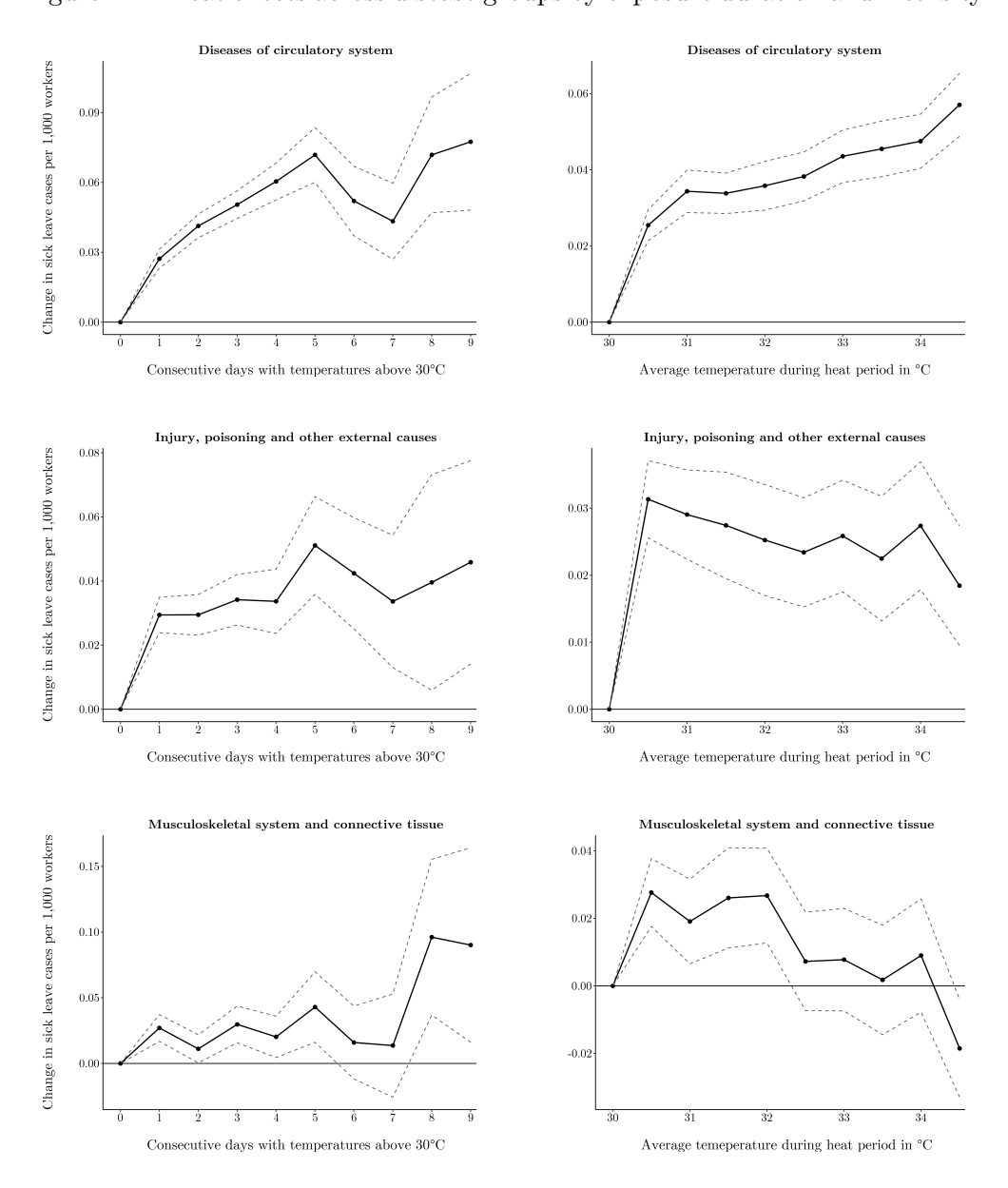
Table A.14: Pooled long-term effect of heat wave exposure

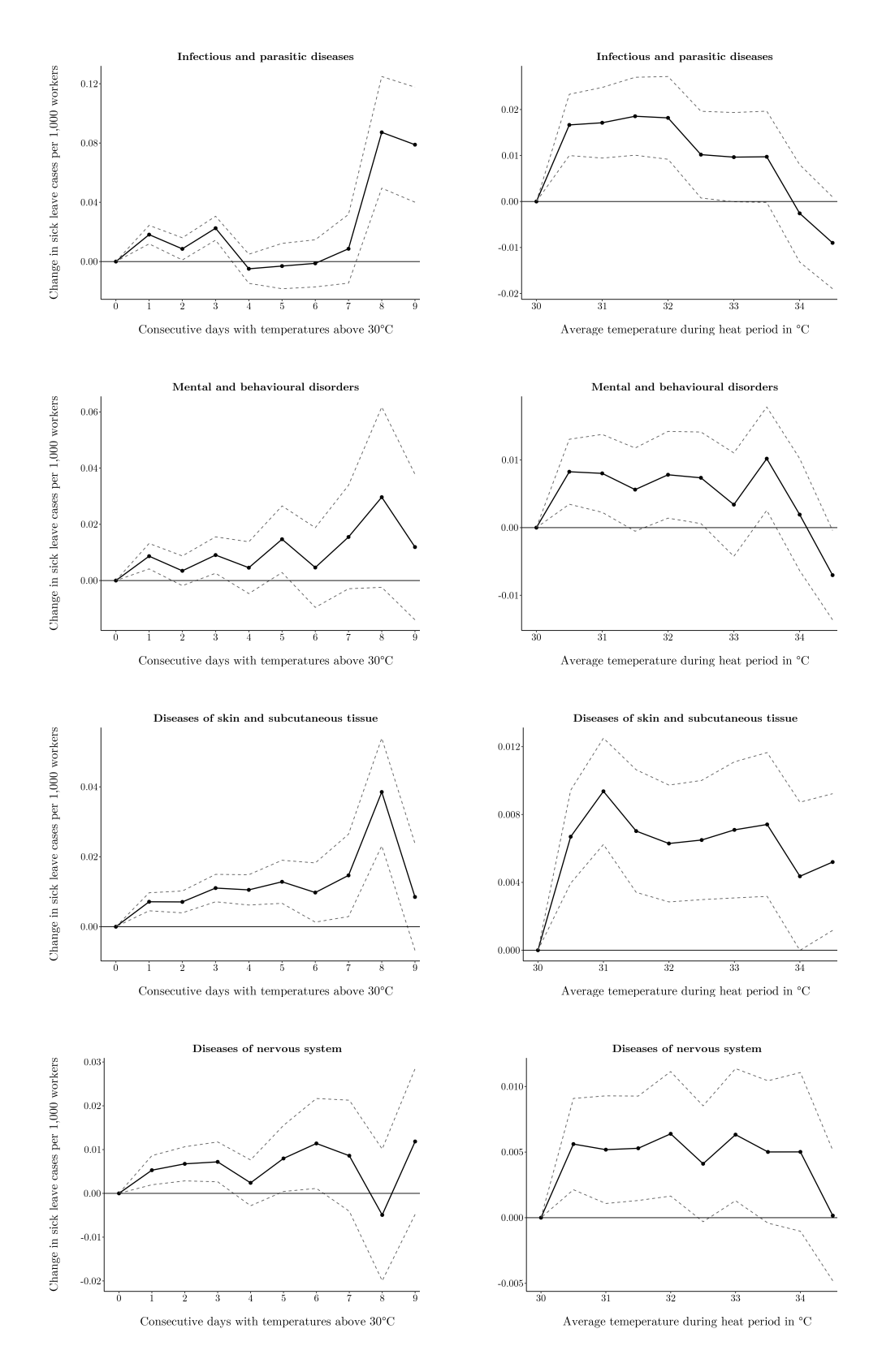
	Expenditures for sick leave compensation	Expenditures for doctor visits
	(in Euro)	(in Euro)
	A. Average effect of heat way	ve day across risk groups
	(1)	(2)
All risk groups	904.911***	41.364*
s.e.	(228.207)	(19.502)
r.e.	[0.221]	[0.035]
	B. Effect of heat wave	day by risk groups
	(3)	(4)
Risk group 1-3	776.394***	24.349
s.e.	(227.845)	(19.938)
r.e.	[19.267]	[0.020]
Risk group 4	2,347.360***	197.878***
s.e.	(286.816)	(43.023)
r.e.	[58.253]	[0.166]
Risk group 5	4,682.843***	627.613***
s.e.	(367.717)	(59.022)
r.e.	[116.211]	[0.526]
Risk group 6	9,613.696***	1,203.578***
s.e.	(1,502.208)	(237.138)
r.e.	[238.577]	[1.009]

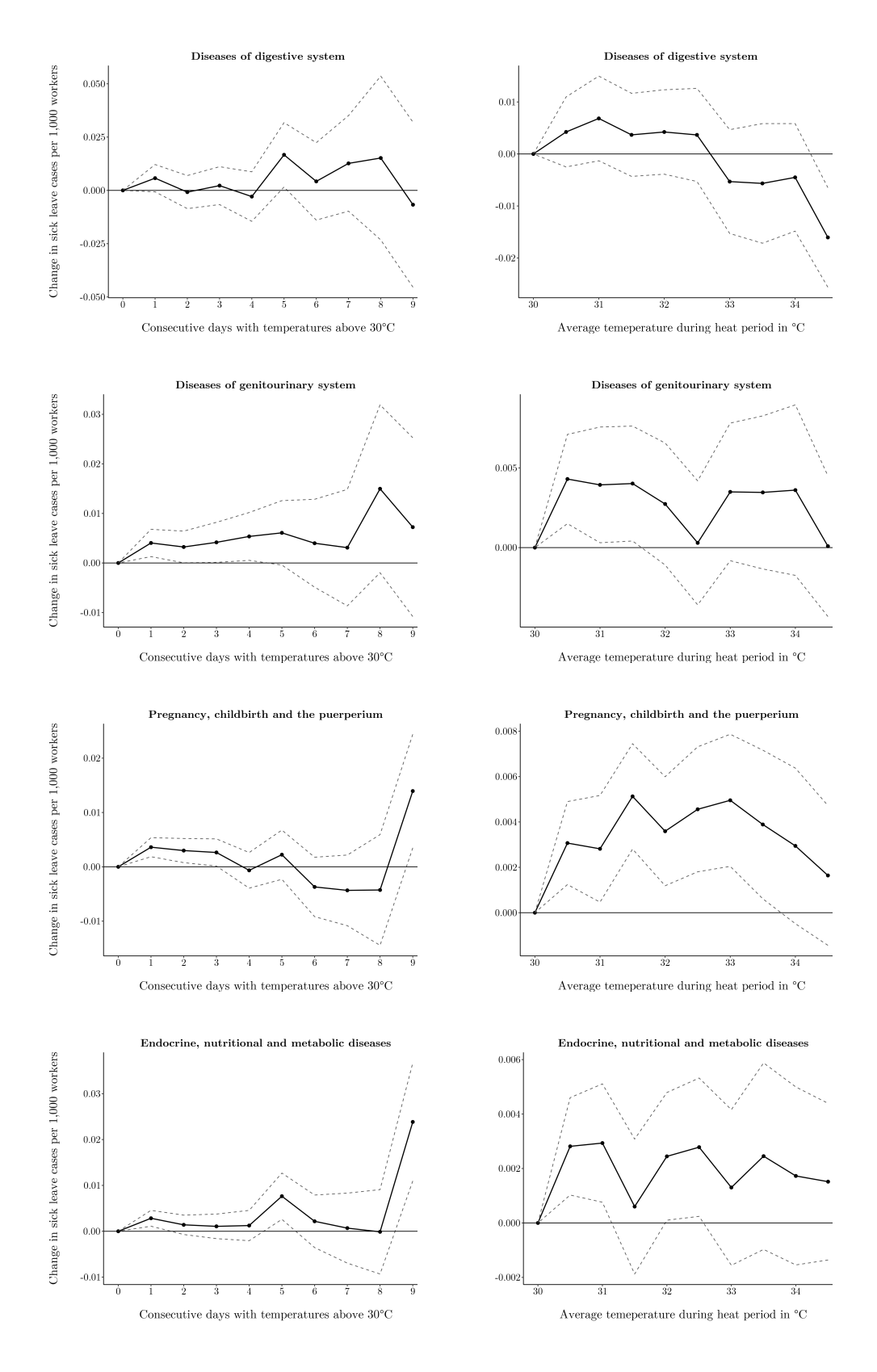
This table reports estimates of the long-term effect of an average heat wave day. The dependent variable refers to either the expenditures (in Euro) for (i) sick leave compensation in the current quarter or (ii) the average number of outpatient treatments by a doctor over the previous eight quarters, both measured per 1,000 workers and quarter. Risk group 1-3 refers to workers with a predicted heat-absence risk in the [0,90) percentile-interval, risk group 4 to the [90,95), risk group 5 to the [95,99), and risk group 6 to the [99, 100] percentile-interval, respectively. The regressions include zip area-year and state-year-quarter fixed effects. We include controls for sex and precipitation. The regressions are weighted by the number of workers per zip-sex-risk group cell. Standard errors in round parentheses are clustered at the county level. Relative effects in percent are in square parentheses. The sample size is 935,579. * p < .05, ** p < .01, *** p < .001.

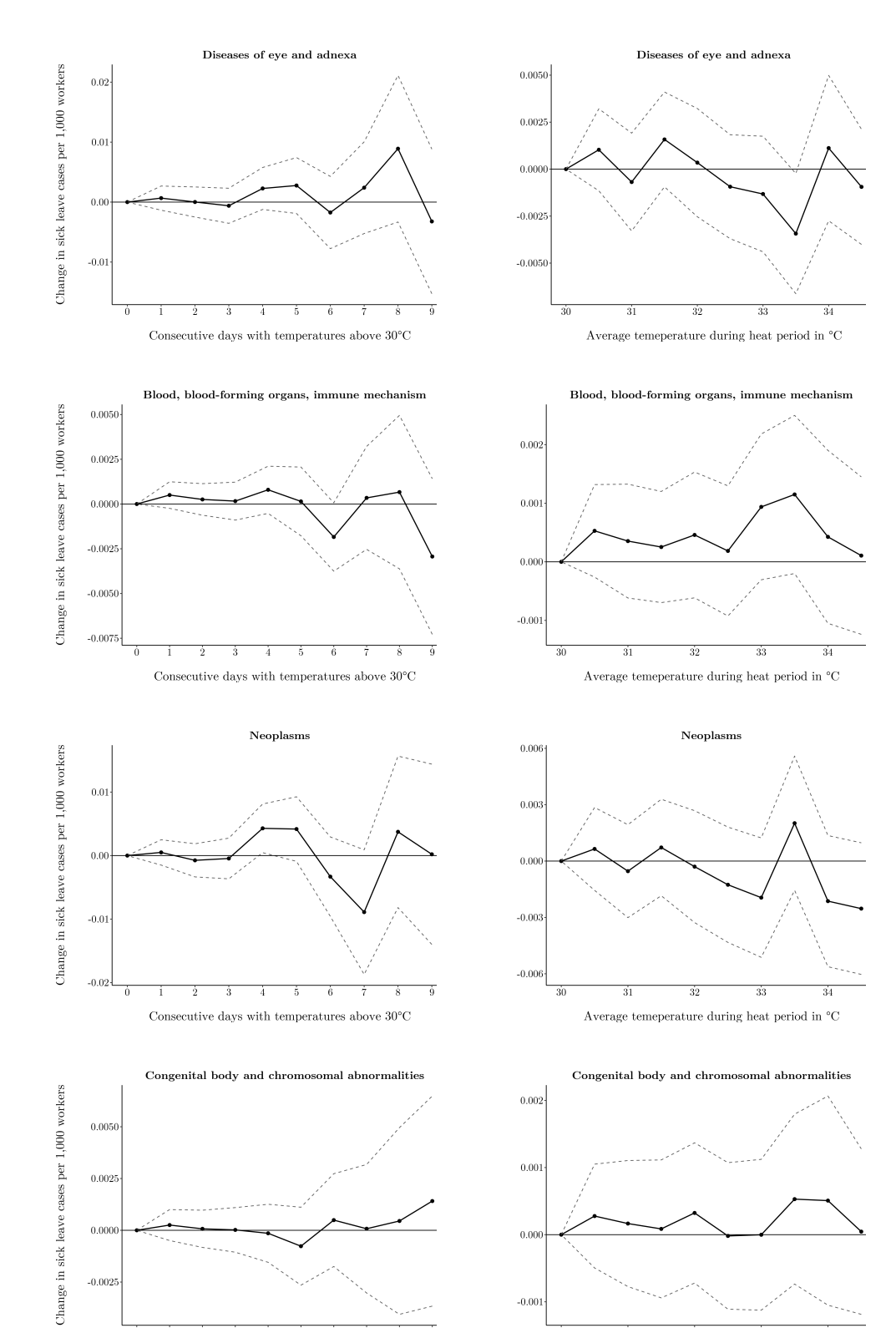
B Figures

Figure B.1: Heat effects across disease groups by exposure duration and intensity





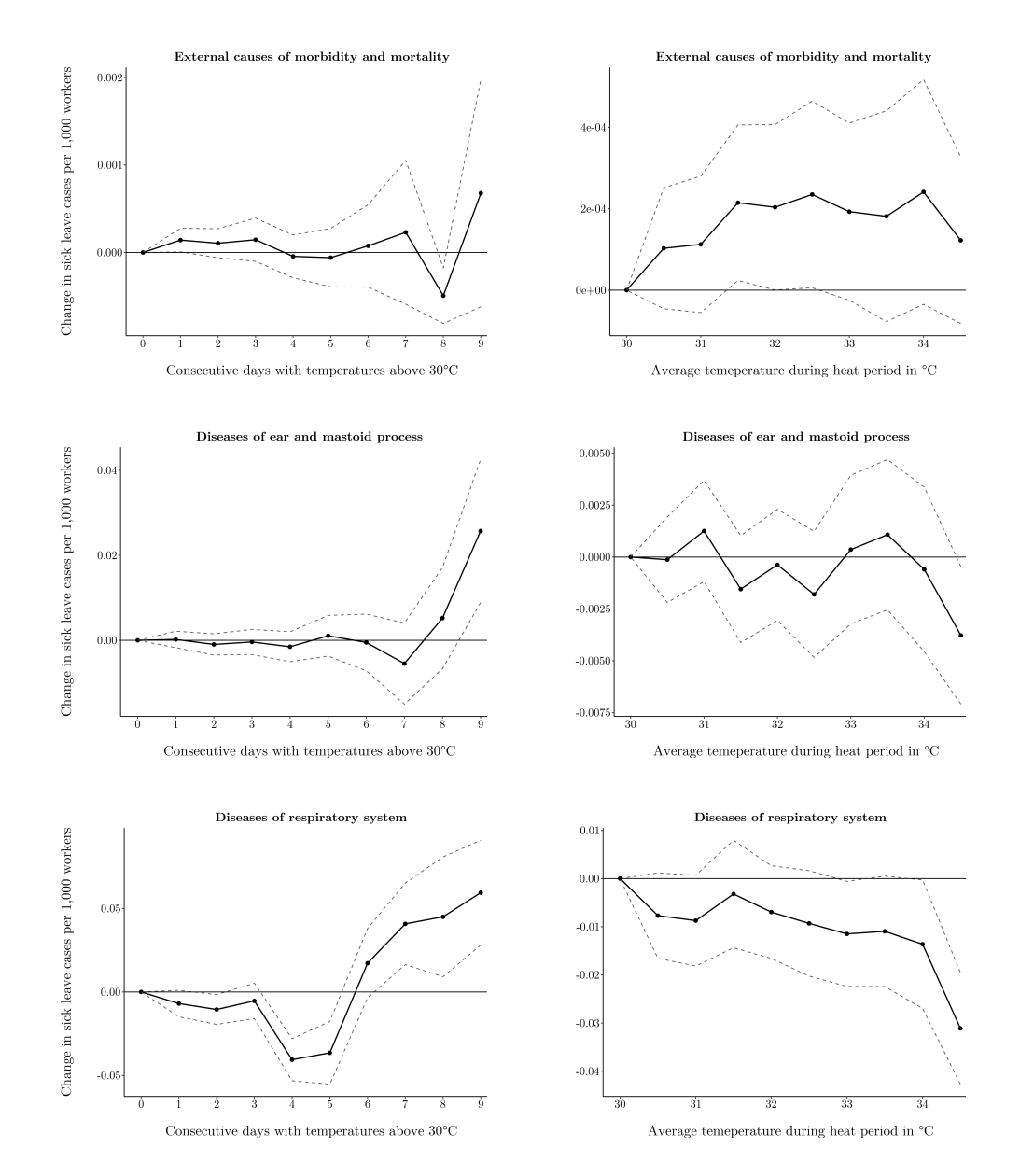




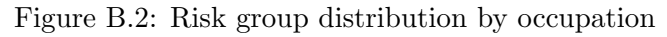
Average temeperature during heat period in ${\rm ^{\circ}C}$

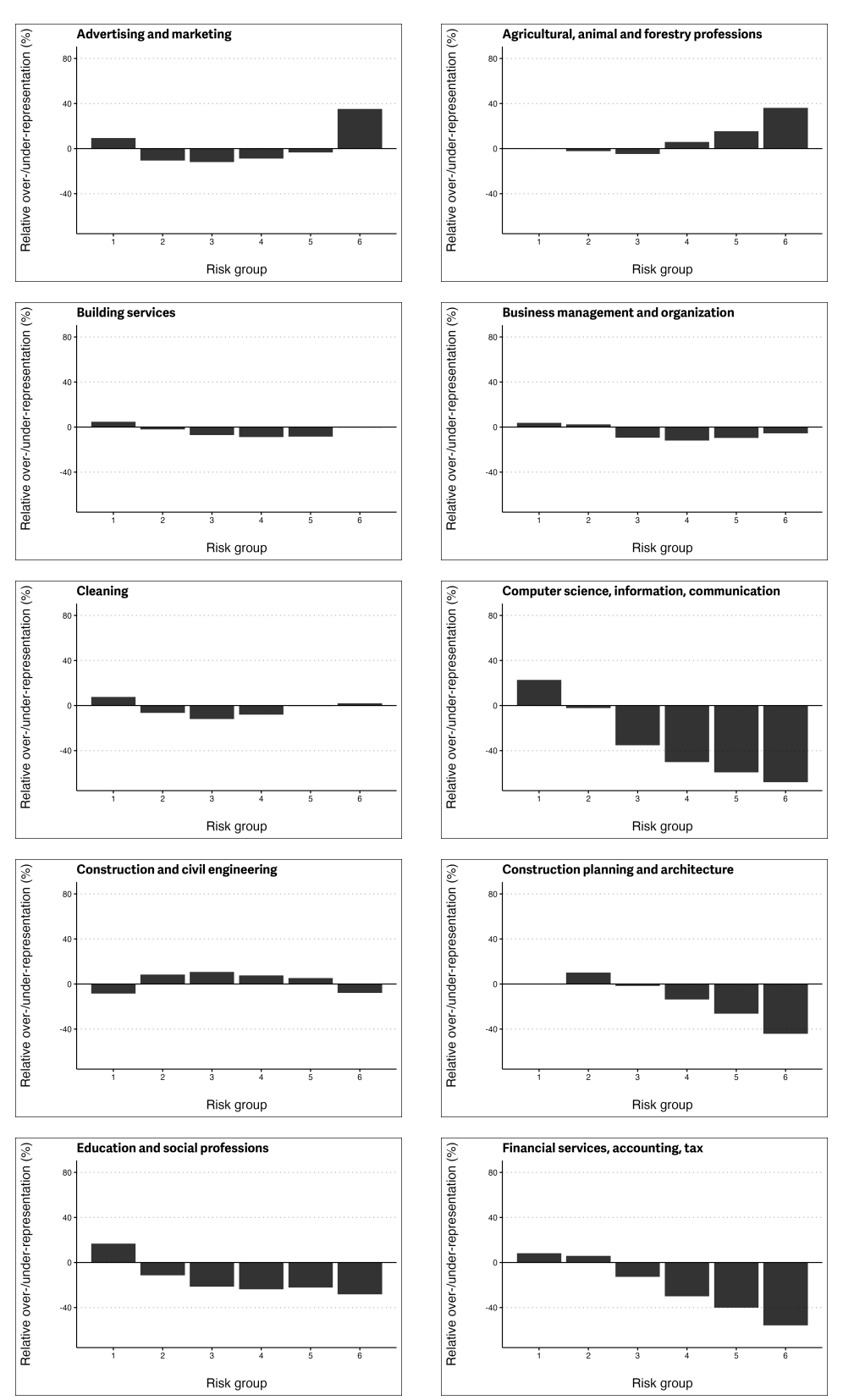
-0.0025

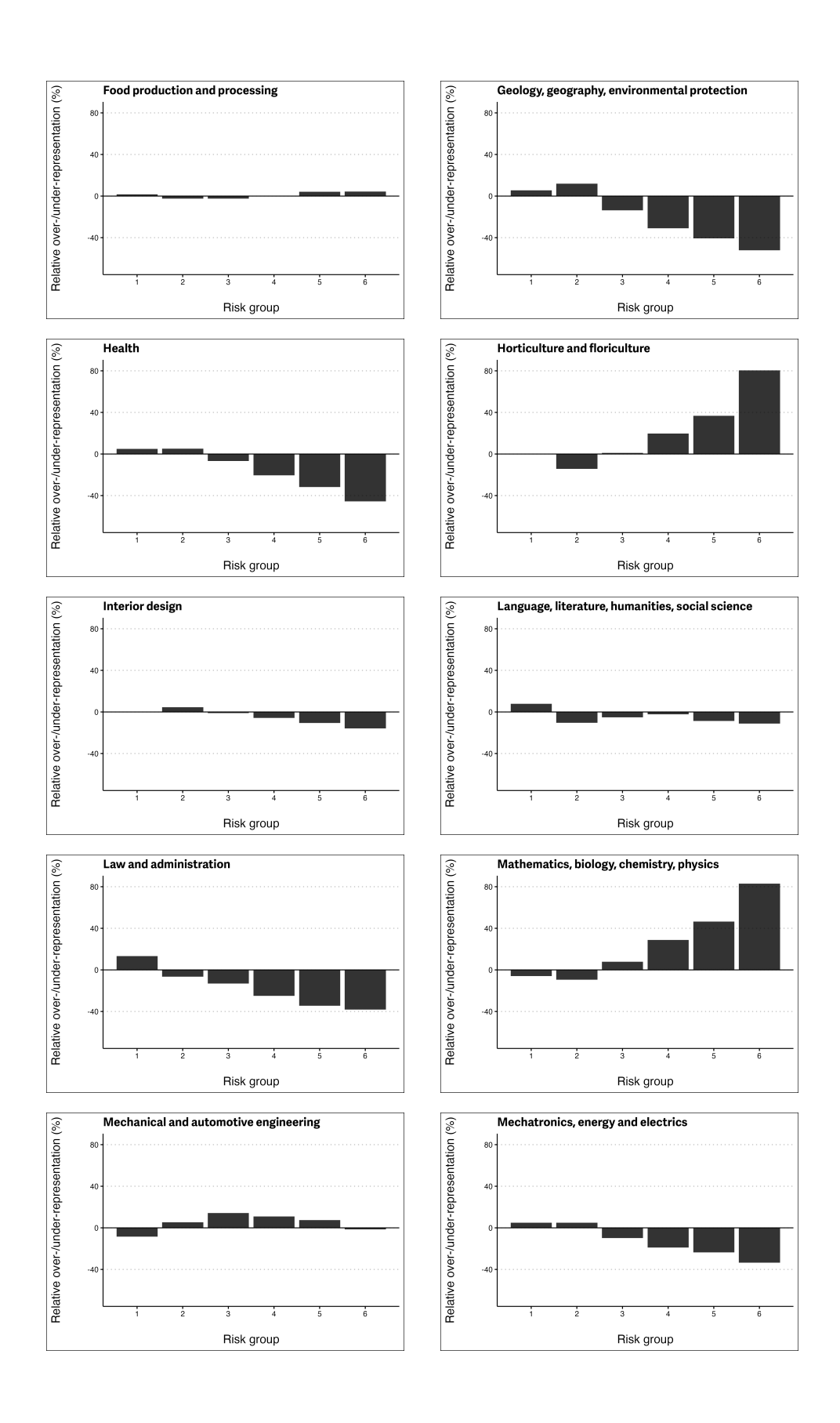
Consecutive days with temperatures above $30^{\circ}\mathrm{C}$

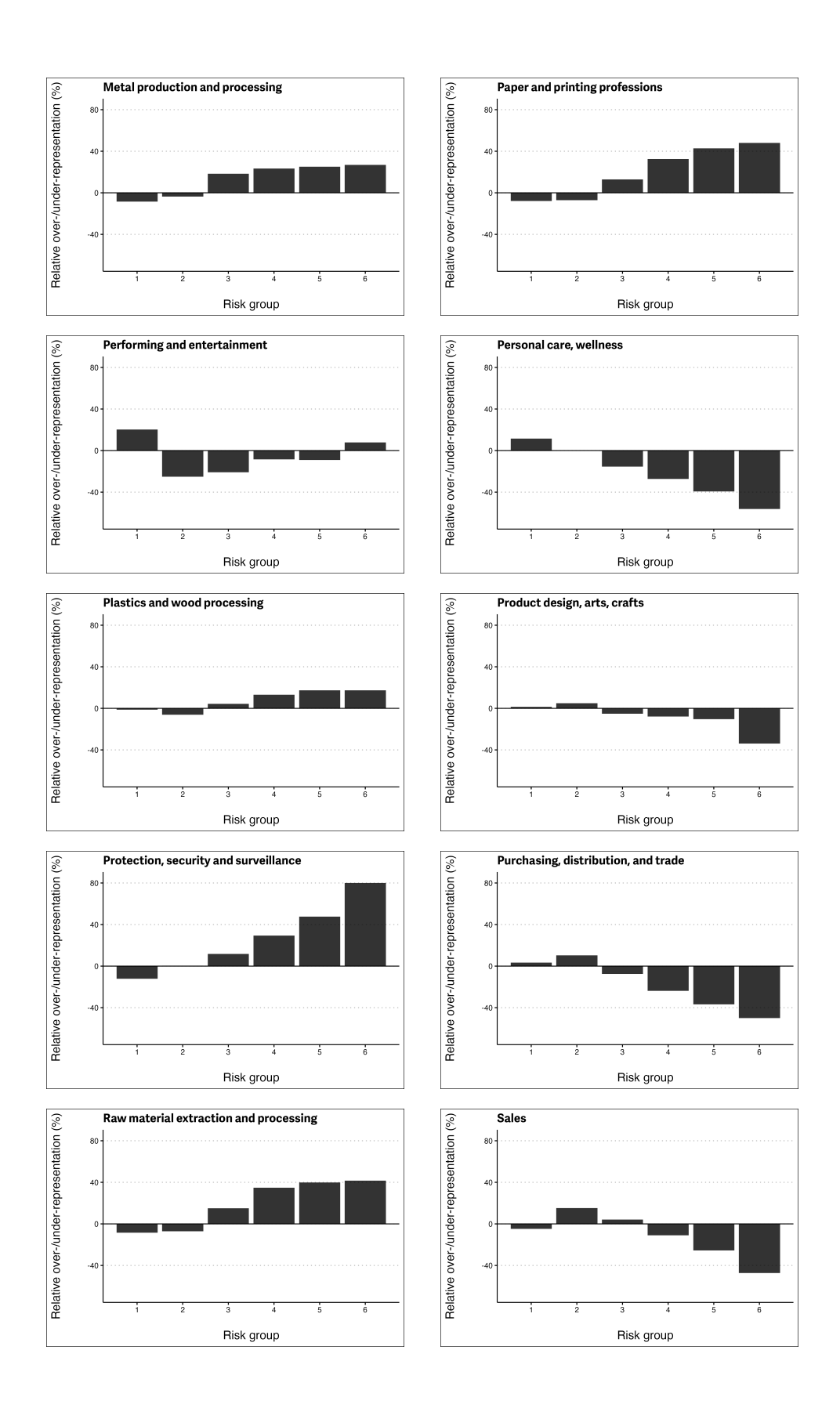


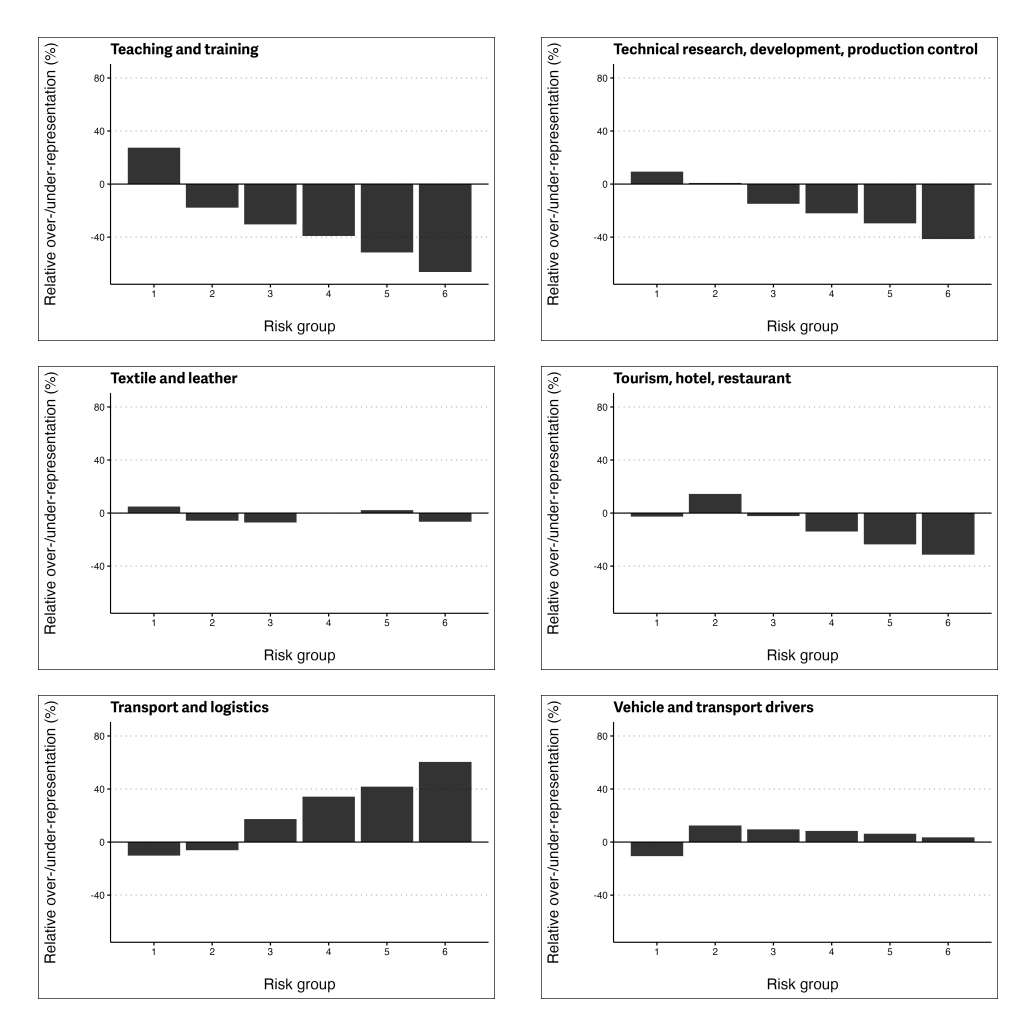
The figure illustrates how the effects of heat vary by duration (i.e. the number of consecutive heat days) and intensity of exposure (i.e. the average temperature of a heat period). The dependent variable is the number of new sick leave cases per 1,000 workers, specific to the disease group indicated in each subplot title. The regressions include zip area—month, year—week, day-of-the-week—month, and day-of-the-year fixed effects. We include controls for age, sex, public holidays, and precipitation. The regressions are weighted by the number of workers per zip-age-gender cell. Standard errors are clustered at the county level. Confidence intervals refer to the 5% level of significance.





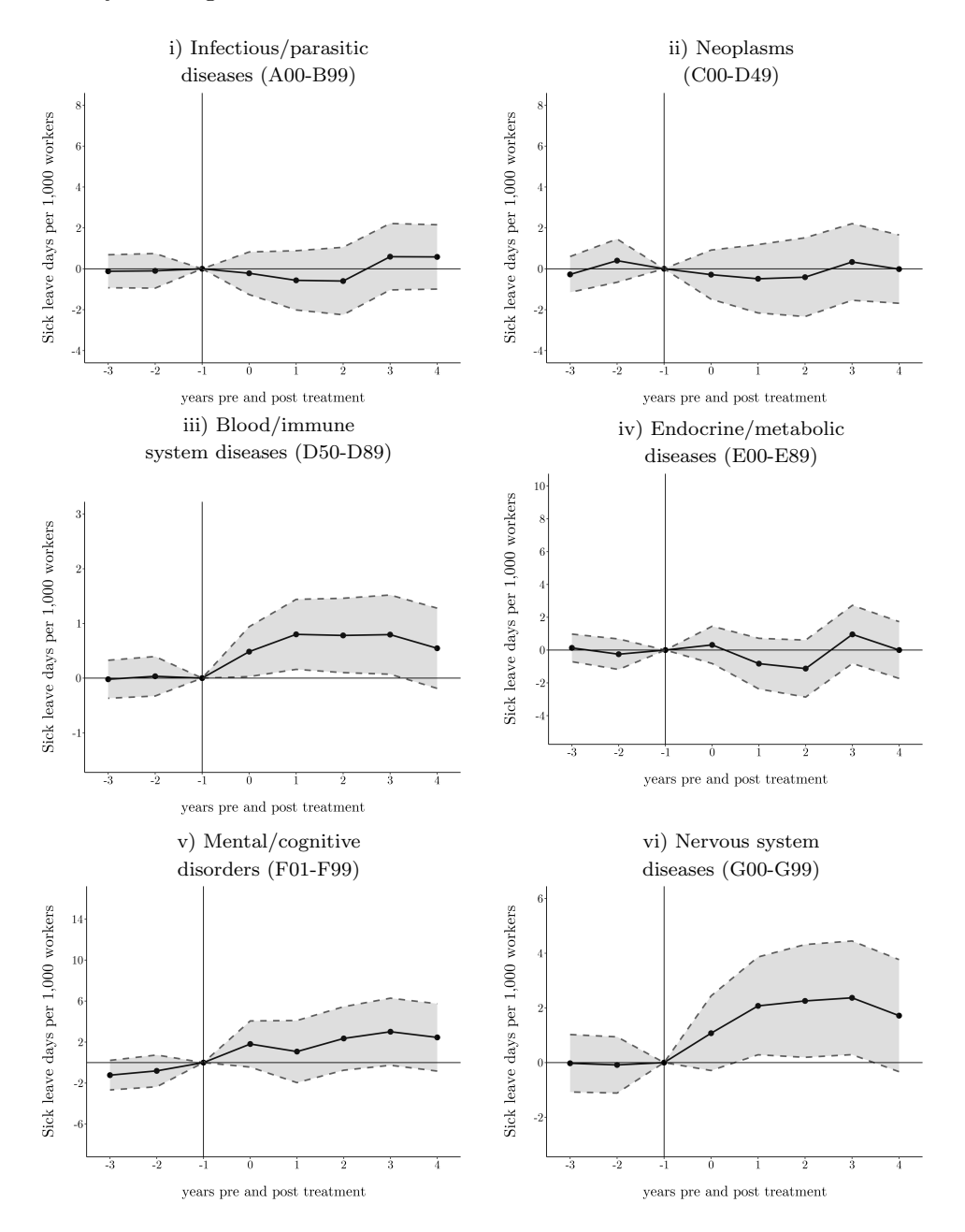


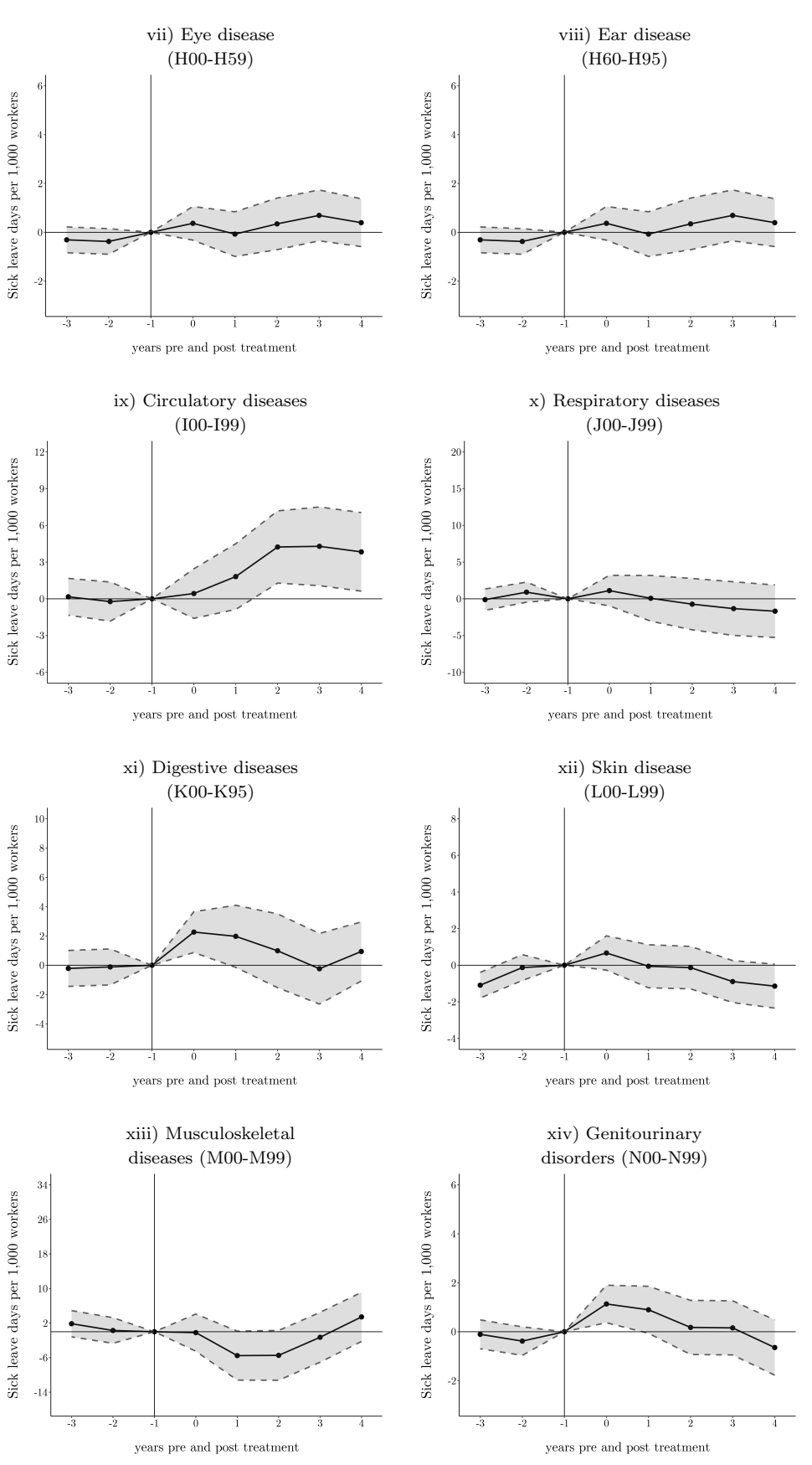


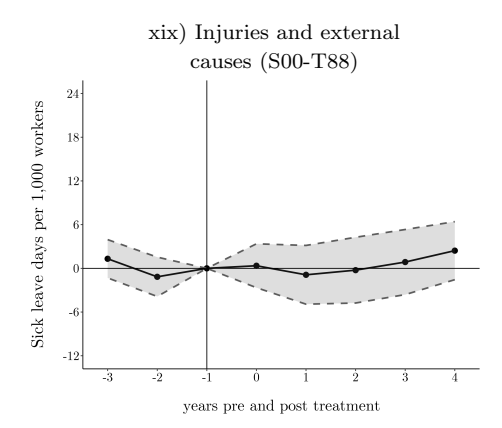


This figure displays the distribution of workers across risk groups for every occupation group. Occupation groups are classified by the 2-digit KldB code and shown in each subplot title. Bars show each risk group's relative deviation, in percent, from the mean share of workers in that risk group across all occupations. Positive values indicate overrepresentation in the occupation, while negative values indicate underrepresentation. For example, a value of 20% for Risk Group 1 means that the share of workers with the lowest heat-absence risk is 20% higher relative to the overall mean across all occupations.

Figure B.3: Event-study estimates of heat wave effects on cause-specific sick leave days among male workers

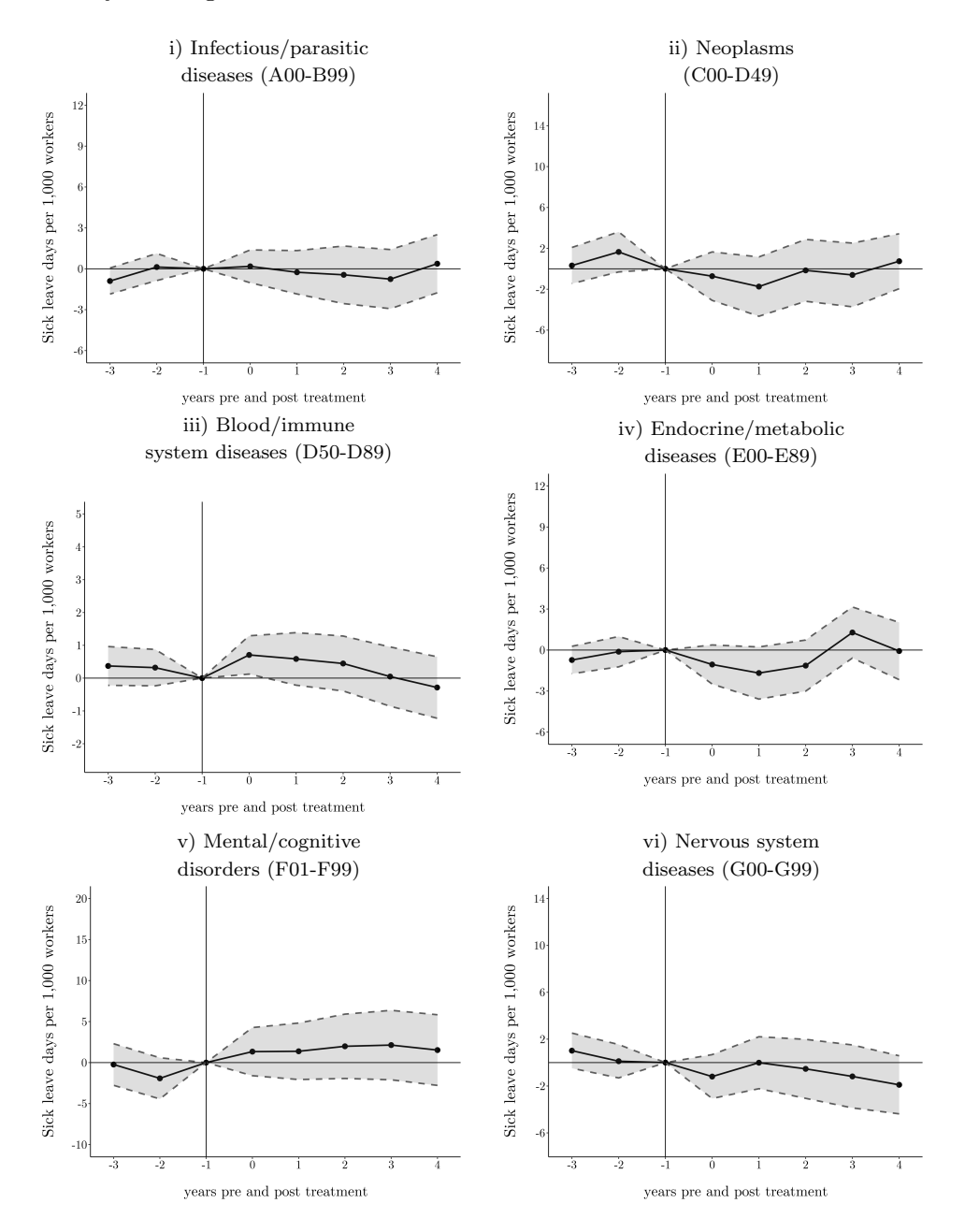


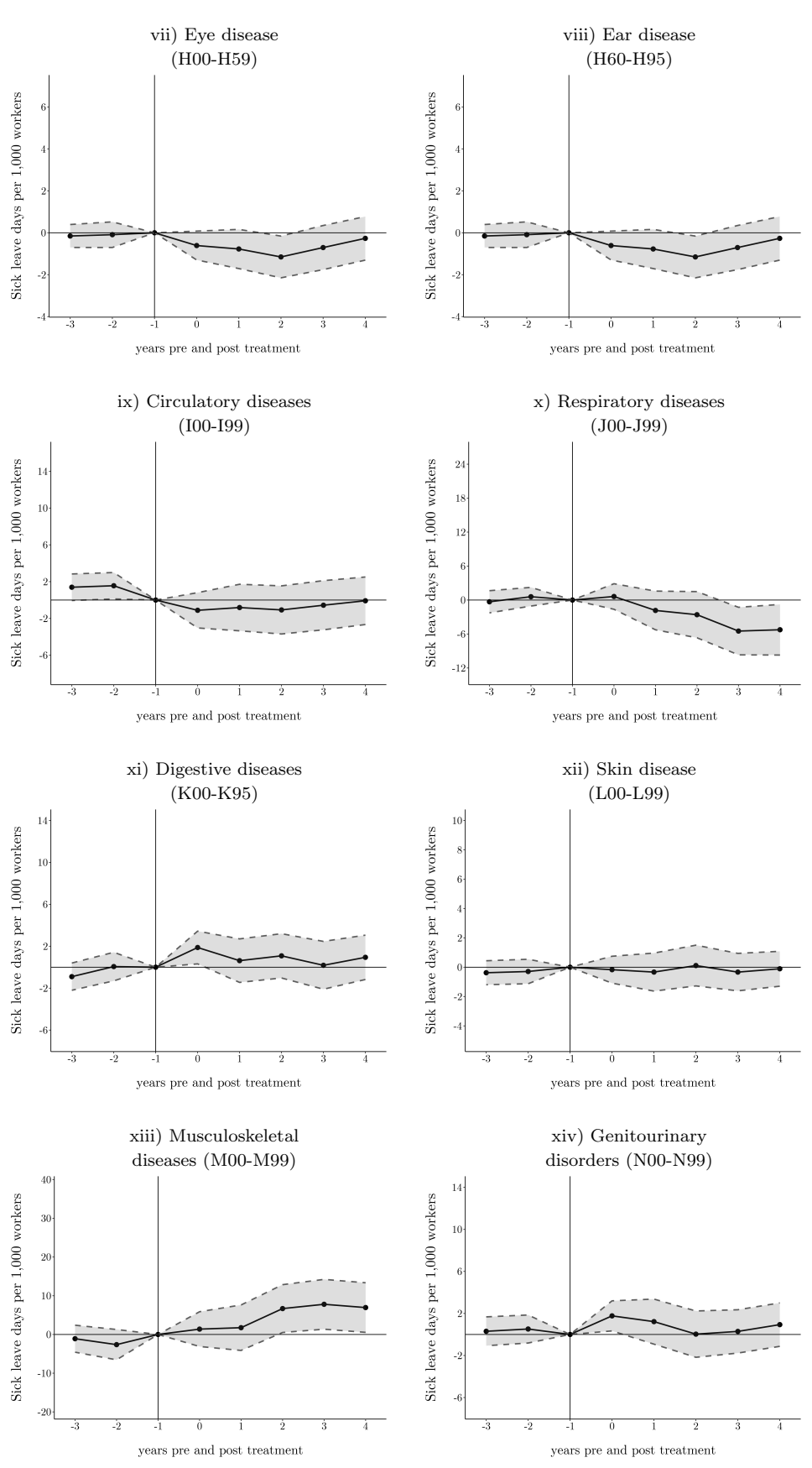


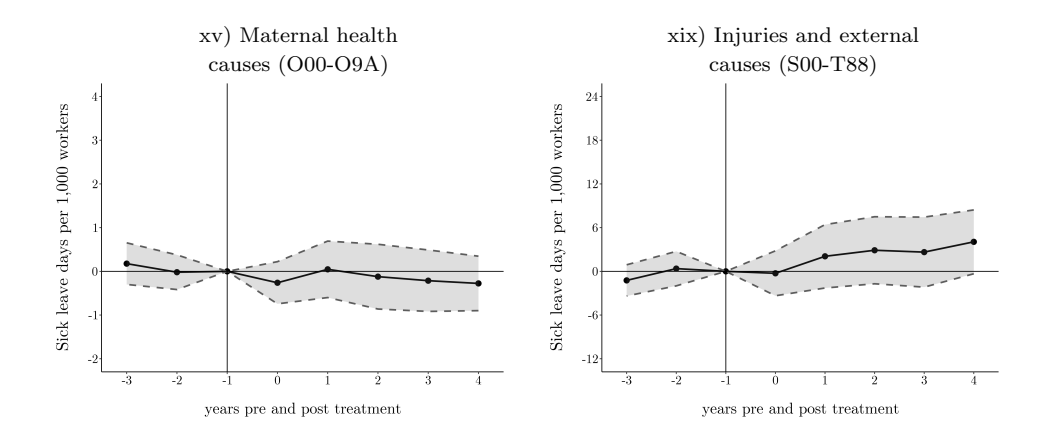


This figure illustrates the effects of heat wave days in the years prior and post to exposure among male workers. The dependent variable refers to the number of cause-specific sick leave days per 1,000 workers and quarter. The regressions include zip area—year and state—year—quarter fixed effects. We include controls for sex and precipitation. The regressions are weighted by the number of workers per zip-sex-risk group cell. Standard errors are clustered at the county level. The sample size is 935,579. Confidence intervals refer to the 5% level of significance.

Figure B.4: Event-study estimates of heat wave effects on cause-specific sick leave days among female workers

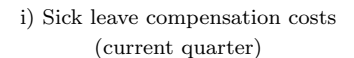


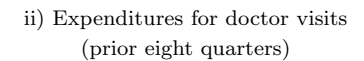


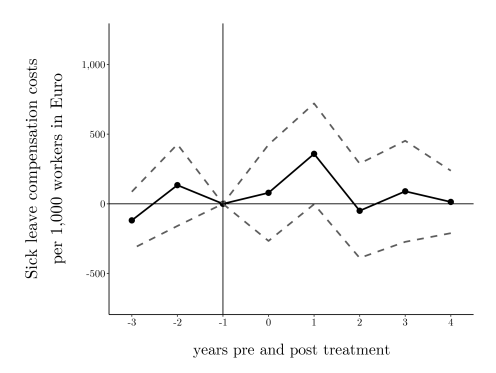


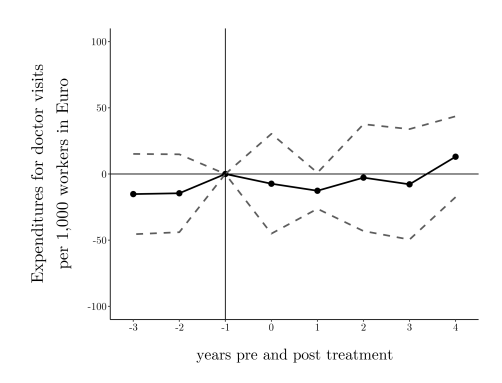
This figure illustrates the effects of heat wave days in the years prior and post to exposure among female workers. The dependent variable refers to the number of cause-specific sick leave days per 1,000 workers and quarter. The regressions include zip area—year and state—year—quarter fixed effects. We include controls for sex and precipitation. The regressions are weighted by the number of workers per zip-sex-risk group cell. Standard errors are clustered at the county level. The sample size is 935,579. Confidence intervals refer to the 5% level of significance.

Figure B.5: Placebo event-study estimates of long-term effects of heat waves









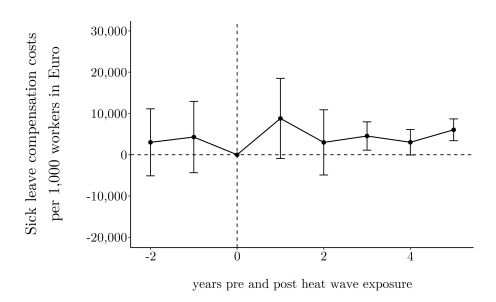
This figure illustrates the placebo effects of heat wave days in the years prior and post to exposure. The dependent variable refers to either the expenditures (in Euro) for (i) sick leave compensation in the current quarter or (ii) the average number of outpatient treatments by a doctor over the previous eight quarters, both measured per 1,000 workers and quarter. The regressions include zip area-year and state-year-quarter fixed effects. We include controls for sex and precipitation. The regressions are weighted by the number of workers per zip-sex-risk group cell and the treatment variable is randomized across the zip-sex-risk group cells. Standard errors are clustered at the county level. Confidence intervals refer to the 5% level of significance.

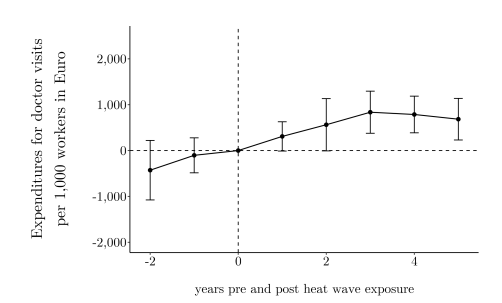
Figure B.6: Event-study estimates of long-term effects of heat waves on health

- i) Sick leave compensation costs (current quarter)
- ii) Expenditures for doctor visits (prior eight quarters)

Average total effect: $15,675.172^{***}(4,269.675)$

Average total effect: $2,177.690^{***}(649.363)$





This figure illustrates the effects of heat wave days in the years prior and post to exposure using the estimator robust to heterogeneous treatment effects proposed by De Chaisemartin and d'Haultfoeuille (2024). We estimate event-study effects that are normalized by the average cumulative incremental treatment dose received, and restrict the estimation to switchers for which all effects can be estimated, to avoid compositional changes. The dependent variable refers to either the expenditures (in Euro) for (i) sick leave compensation in the current quarter or (ii) the average number of outpatient treatments by a doctor over the previous eight quarters, both measured per 1,000 workers and year. The data are aggregated to the year-zip level and the regressions include zip and state—year fixed effects. We include controls for precipitation. The regressions are weighted by the number of workers per zip cell. Standard errors are clustered at the county level. The sample size is 72,862. Confidence intervals refer to the 5% level of significance.

C Implementation of ML-based heterogeneity analysis

Implementing the ML-based heterogeneity analysis involves practical implementation challenges because of the size of the individual-level data. Therefore, we restrict the analyses to observations occurring in the warmer months May through September. Additionally, we train not a single prediction model based on the observations in our control group, but randomly divide the control observations into three subsets and train a separate model on each subset. The predicted control values for the main dataset are then averaged across the three models.

We also account for the relatively low probability of a new sick leave case on any given day and follow Deryugina et al. (2019) by using a downsampling method. Further details on this method are provided in Einav et al. 2018. We then run the regressions on equally sized partitions of the data to aggregate the coefficients and standard errors subsequently. To this end, we split the data randomly into 250 partitions that contain 13,780,187 observations each. To aggregate the results, we calculate the mean of the estimated coefficients and divide the mean of the estimated standard errors by the square root of 250. Due to long computing times, we do not repeat our estimation 100 times as recommended by Chernozhukov et al. (2018) and argue that splitting variation is a minor concern given our large sample sizes (see Deryugina et al. 2019). In all analyses, we include only observations with an estimated propensity score between 0.025 to 0.975 to reduce noise.

D Comparison of effect size with literature on stroke survivors

While suitable benchmarks for our estimates of the long-term effects of heat waves in Section 4.3 are scarce, we aim to provide some context using available literature. To this end, we compare them to the costs occurring for ischemic stroke survivors in post-incident years.

The study by Kolominsky-Rabas et al. (2006) shows that the mean annual healthcare costs per survivor of a stroke in Germany amount to $7{,}012.37\mathfrak{C}$ in the years two through five after the stroke occurred. Of these costs $3{,}433.87\mathfrak{C}$ accumulate for outpatient services like doctor visits and prescriptions.²⁸ The annual costs for doctor visits linked to a three-day heat wave according to our estimates are $0.50\mathfrak{C}$ per worker ($124\mathfrak{C} \cdot 4$ quarters / $1{,}000$ workers). This implies that exposing approximately $6{,}868$ workers ($3{,}433.87\mathfrak{C}$ / $0.50\mathfrak{C}$) to a severe heatwave results in long-term costs for doctor visits comparable to those of all outpatient costs incurred by a single additional stroke survivor.

Moreover, in a study on Denmark, Skajaa et al. (2023) show that in the second year after a stroke, survivors experience a 2.89-fold higher prevalence of sick leave, beyond the baseline rate observed in the general population. Our data reveals that, on average, workers accumulate 17.18 sick leave days per year. The average median income per day across occupation groups is $101.58\mathfrak{C}$. Accordingly, the annual additional sick leave costs linked to a stroke are about $5.043.47\mathfrak{C}$ (2.89 · 17.18 days · $101.58\mathfrak{C}$). The annual per capita costs for sick leave-related income compensation linked to a three-day heat wave according to our estimates are $10.86\mathfrak{C}$ (2.715 \mathfrak{C} /quarter · 4 quarters / 1,000 workers). This implies that exposing approximately 464 workers (5.043.47 \mathfrak{C} / 10.86 \mathfrak{C}) to a severe heatwave results in long-term sick leave costs comparable to those incurred by a single additional stroke survivor.

²⁸Kolominsky-Rabas et al. 2006 report costs of 5,479€ in total and 2,683€ for outpatient services in Germany in 2004 values in their Table 1, which we adjust for inflation to obtain the 2020 values of 7,012.37€ and 3,433.87€.

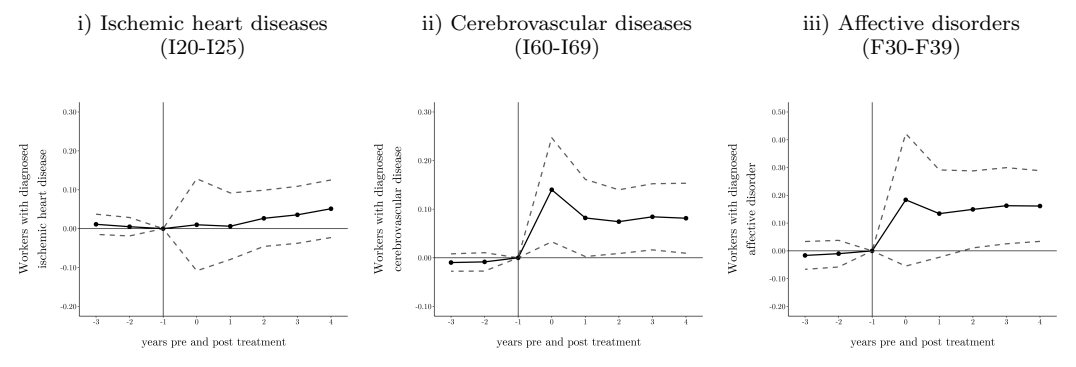
 $^{^{29}\}mathrm{We}$ derive this number from Table 2 in the study by Skajaa et al. 2023.

E Disease-specific extensive margins in long-term heat wave effects

The long-term effects on sick leave and outpatient care documented in Section 4.3 may be driven by several causes. Here, we explore disease-specific channels operating on the extensive margin. To this end, we use available data on the number of workers diagnosed with three selected diseases that typically require long-term treatment: ischemic heart diseases (I20-I25), cerebrovascular diseases such as stroke (I60-I69), and affective disorders such as recurrent depressive episodes (F30-F39). We observe the prevalence of these diseases at a quarterly frequency for each worker recorded over the preceding eight quarters.

Figure E.7 presents event-study estimates with patterns suggesting that heat waves contribute to new diagnoses of workers with cerebrovascular and affective disorders. We also estimate pooled post-treatment effects in Table E.15. Accordingly, for every 1,000 individuals exposed to a three-day heat wave, we observe $0.183~(0.061 \cdot 3)$ additional diagnoses of cerebrovascular diseases which corresponds to an increase of about 1%. Moreover, our results suggest $0.462~(0.154 \cdot 3)$ additional diagnoses of affective disorders, which corresponds to a 0.35% increase. The estimates are economically meaningful and suggest that heat wave exposure can increase the number of diagnosed diseases that often come with longer-term treatment.

Figure E.7: Event-study estimates of heat wave effects on prevalence of specific diagnoses



This figure illustrates the effects of heat wave days in the years prior and post to exposure. The dependent variable refers to the number of workers diagnosed with either (i) cerebrovascular diseases, (ii) ischemic heart diseases, or (iii) affective disorders measured in every quarter over the previous eight quarters per 1,000 workers. The regressions include zip area—year and state—year—quarter fixed effects. We include controls for sex and precipitation. The regressions are weighted by the number of workers per zip-sex-risk group cell. Standard errors are clustered at the county level. The sample size is 935,579. Confidence intervals refer to the 5% level of significance.

Table E.15: Pooled post-treatment effect of heat waves on prevalence of specific diagnoses

	Workers diagnosed per 1,000 workers		
	Ischemic heart disease (I20-I25) (1)	Cerebrovascular disease (I60-I69) (2)	Affective disorder (F30-F39) (3)
Heat wave day	0.049	0.061*	0.154**
s.e.	(0.032)	(0.03)	(0.057)
r.e.	[0.137]	[0.331]	[0.116]

This table reports estimates of the effect of an average heat wave day on the prevalence of specific diseases. The dependent variable refers to the number of workers diagnosed with either (i) ischemic heart disease, (ii) cerebrovascular disease, or (iii) affective disorder measured in every quarter over the previous eight quarters per 1,000 workers. The regressions include zip area-year and state-year-quarter fixed effects. We include controls for sex and precipitation. The regressions are weighted by the number of workers per zip-sex-risk group cell. Standard errors are clustered at the county level. The sample size is 935,579. Confidence intervals refer to the 5% level of significance. Standard errors in round parentheses are clustered at the county level. Relative effects in percent are in square parentheses. The sample size is 935,579. * p < .05, *** p < .01, **** p < .001.

We argue that the findings speak to the existence of two possible channels on the extensive margin. First, heat waves trigger the onset of new conditions, representing significant health shocks that can persistently impair workers' health and ability to work. This is especially relevant for cerebrovascular diseases (I60-I69), which predominantly involve acute, sudden-onset events such as strokes and hemorrhages. Although some underlying vascular pathologies may develop gradually over time, the transition to clinically manifest events that lead to diagnosis and necessitate long-term treatment is typically abrupt and severe. Extended care is common in these cases. In particular, stroke survivors often require rehabilitation and ongoing medical support due to lasting physical, cognitive, or functional impairments (see Section D). Second, heat waves may temporarily exacerbate existing symptoms, prompting individuals to seek medical attention and leading to the diagnosis of preexisting but previously undetected conditions. This channel is particularly relevant for mental health, where prior research has demonstrated a robust association between heat exposure and worsening psychological outcomes (Mullins and White 2019, Obradovich et al. 2018, Burke et al. 2018). In line with this evidence, heat waves may intensify mental health symptoms to the point of clinical recognition, resulting in new diagnoses among individuals who had not previously engaged with the healthcare system. Among mood disorders (F30-F39), the most common diagnoses, such as depressive and recurrent depressive episodes, typically

develop gradually. In such cases, heat-induced symptom aggravation may serve as a catalyst for diagnosis rather than indicating the onset of entirely new mental illnesses, highlighting a potential role of extreme temperatures in revealing latent disease burdens.

F Long-term heat wave effects on pharmaceutical and hospital admission expenditures

In this section, we study the impact of heat waves on two additional outcome variables measuring healthcare demand. The first variable is the number of distinct pharmaceuticals prescribed over the previous eight quarters, identified at the three-digit code of the Anatomical Therapeutic Chemical (ATC) classification system for pharmaceuticals.³⁰³¹ Similar to the doctor visit outcome variable discussed in Section 2.2, this variable is available only in biannual aggregates, and the exact timing of prescriptions within each period is unknown. Interpretation is further complicated by the fact that, although the variable measures the number of distinct pharmaceuticals a patient receives over an eight-quarter period, it does not account for prescription frequency, i.e., whether each pharmaceutical is prescribed only once or on multiple occasions across quarters. Consequently, the variable should be viewed as reflecting the level of co-morbidity by capturing the diversity of conditions requiring pharmaceutical treatment. It does not provide information on the severity of morbidity, which may stem from multiple conditions or a single disease. To adopt a conservative approach, we assume each distinct pharmaceutical is prescribed only once over the observed eight quarters, dividing the variable by eight to approximate a quarterly measure. We then multiply this quarterly estimate by 64.02€, the average cost per pharmaceutical prescription in 2020 values (Wissenschaftliches Institut der AOK 2020).

The second outcome is the number of hospital treatments with distinct discharge diagnoses in the previous quarter, identified at the three-digit ICD-10 code level.³² This variable is reported quarterly; however, similar to the prescription outcome, it does not capture repeated hospital admissions for the same ICD diagnosis. To obtain a cost estimate, we multiply this variable by 5,125.77€, representing the average cost per hospitalization in 2020 values (Destatis 2021).

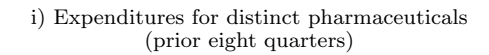
Because both variables capture only specific aspects of pharmaceutical and hospital treatment demand, their interpretation is not straightforward, and we therefore exclude

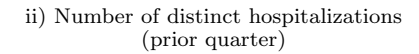
³⁰The ATC classification system categorizes drugs based on their active ingredients according to the organ or the system on which they act as well as their therapeutic, pharmacological, and chemical properties.

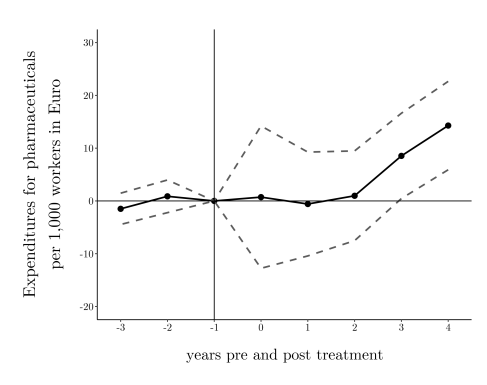
³¹We include this variable also as input feature in the gradient-boosted decision tree model described in Section 3.2.

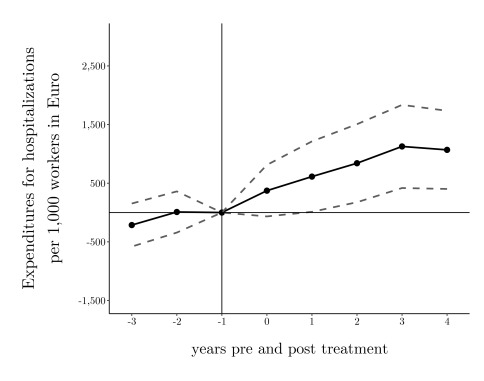
³²We include this variable also as input feature in the gradient-boosted decision tree model described in Section 3.2.

Figure F.8: Event-study estimates of long-term effects of heat waves on expenditures for pharmaceuticals and hospitalizations









This figure illustrates the effects of heat wave days in the years prior and post to exposure. The dependent variable refers to either the expenditures (in Euro) for (i) the average number of distinct pharmaceuticals prescribed over the previous eight quarters or (ii) the number of hospital treatments with distinct discharge diagnoses in the previous quarter, both measured per 1,000 workers and quarter. The regressions include zip area—year and state—year—quarter fixed effects. We include controls for sex and precipitation. The regressions are weighted by the number of workers per zip-sex-risk group cell. Standard errors are clustered at the county level. Confidence intervals refer to the 5% level of significance.

them from our main analysis. However, for readers interested in these outcomes, we re-estimate Figure 9 using them as dependent variables. Figure F.8 reveals statistically significant post treatment effects for both outcomes, however only in the later years of the observed time period. Moreover, applying the robust estimator proposed by De Chaisemartin and d'Haultfoeuille (2024), we find no statistically significant treatment effects for either outcome.